# REPORT DOCUMENTATION PAGE

AFRL-SR-BL-TR-98-

0660

Public reporting burden for this collection of information is estimated to average 1 [illegible] per response, including the ti
gathering and maintaining the data needed, and completing and reviewing the co[illegible]on of information. Send comme
collection of information, including suggestions for reducing this burden, to Washington Headquarters Services, Direct
Davis Highway, Suite 1204, Arlington, VA 22202-4302, and to the Office of Management and Budget, Paperwork Reduction

| | | |
|---|---|---|
| 1. AGENCY USE ONLY *(Leave Blank)* | 2. REPORT DATE<br>23 Sep 98 | 3. REPORT TYPE AND DATES COVERED<br>Final Report 01 Sep 93 through 28 Feb 98 |

4. TITLE AND SUBTITLE
Instrumentation to Enhance Optical Scatterometry for Semiconductor Metrology Development

5. FUNDING NUMBERS
F49620-93-1-0512

6. AUTHORS
J. R. McNeil

7. PERFORMING ORGANIZATION NAME(S) AND ADDRESS(ES)
The University of New Mexico
Center for High Technology Materials
1313 Goddard SE
Albuquerque, NM 87106

8. PERFORMING ORGANIZATION REPORT NUMBER
FR 329361

9. SPONSORING / MONITORING AGENCY NAME(S) AND ADDRESS(ES)
Air Force Office of Scientific Research/NE
110 Duncan Ave, Suite B115
Bolling AFB, DC 20332-8080

10. SPONSORING / MONITORING AGENCY REPORT NUMBER

11. SUPPLEMENTARY NOTES

12a. DISTRIBUTION / AVAILABILITY STATEMENT
UNL

12b. DISTRIBUTION CODE

13. ABSTRACT *(Maximum 200 words)*

This Equipment Grant enabled upgrades in our scatterometer research instrumentation and computational capability. This provided a unique capability to develop the metrology technique through performing collaborative investigations with SEMATECH, Texas Instruments, and IBM. These efforts demonstrated the potential of scatterometry to provide the semiconductor industry with a metrology tool for characterizing sub-0.1 m (and larger) features.

14. SUBJECT TERMS
Metrology, Scatterometry

15. NUMBER OF PAGES
23

16. PRICE CODE
NSP

| | | | |
|---|---|---|---|
| 17. SECURITY CLASSIFICATION OF REPORT<br>UNCLASSIFIED | 18. SECURITY CLASSIFICATION OF THIS PAGE<br>UNCLASSIFIED | 19. SECURITY CLASSIFICATION OF ABSTRACT<br>UNCLASSIFIED | 20. LIMITATION OF ABSTRACT<br>UNL |

# INSTRUMENTATION TO ENHANCE OPTICAL SCATTEROMETRY FOR SEMICONDUCTOR METROLOGY

## FINAL REPORT

## SCATTEROMETRY OVERVIEW

Optical scatterometry research at the University of New Mexico (UNM) has involved measurement and analysis of laser diffraction from samples to determine the dimensional and optical characteristics of the sample. This work has resulted to provide the semiconductor industry a simple, repeatable metrology technique applicable to characterizing sub-0.1 µm geometries. Work on scatterometry was initiated in 1990 under support from SEMITECH / SRC, continued until 1996, and has since been supported by Bio-Rad Laboratories. The scatterometer technique has distinct advantages compared to other metrology techniques, including being applicable to small (sub-0.1 µm) dimensions, simple, repeatable, nondestructive, rapid, and based upon fundamental principles (e.g., Maxwell's equations). The semiconductor industry, as expressed in the National Technology Roadmap for Semiconductors, recognizes the need for improved, novel metrology techniques to carry the industry into the next century and the capability of scatterometry to fulfill this need.

## ENABLING BENEFITS OF THE EQUIPMENT GRANT

At the beginning of the period of performance of this Equipment Grant, the scatterometer effort at UNM was well established theoretically. However, the effort utilized equipment that was out-dated and not amenable to investigating state-of-the-art samples for the semiconductor industry. The Equipment Grant permitted a number of significant improvements, primarily computational capabilities, wafer manipulation capability, and incorporation of multiple laser wavelengths. The primary results of incorporating these improvements included the design and execution of two major experiments performed in collaboration with SEMATECH, Texas Instruments, and IBM. The results of these two efforts demonstrated the capabilities of the scatterometer technique to the semiconductor community, which has subsequently led to acceptance of the technique.

**SUB-0.20 µm Photoresist Characterization:** One of the efforts simulated the conditions that would be encountered by applying scatterometer measurement techniques in a semiconductor fabrication environment to characterize photoresist structures with line-widths between 0.15 µm and 0.40 µm. The photoresist was on top of films of poly-Si and $SiO_2$ (i.e. a gate-layer structure). The line-widths of the photoresist structure, the photoresist thickness, and the thicknesses of the other two films were intentionally made

DTIC QUALITY INSPECTED 4

19981006 148

to be different from sample-to-sample, thereby simulating actual fabrication conditions. We demonstrated the ability of scatterometry to provide line-width measurements in a situation in which the thickness of the three layers was changing. Indeed, the single scatterometer measurement provided values of the three thicknesses. This effort was performed in collaboration with investigators at SEMATECH and Texas Instruments, with confirming sample measurements performed at these facilities by other techniques (SEM, AFM, and ellipsometry). Over 3000 sample measurements were performed in this effort, which would not have been possible without the automation and computational enhancements to our scatterometer apparatus provided by the Equipment Grant.

**DRAM Deep Trench Measurement:** We utilized part of the funds of the Equipment Grant to construct a scatterometer arrangement based upon image processing analysis of diffraction data. This provided the ability to perform an effort in collaboration with IBM that involved measurement of deep trenches used in the fabrication of 16 MB DRAM's. The trenches were approximately 8-10 μm deep and had sub-μm oval top profile. This makes it possible to characterize the trenches using only cross-section SEM prior to our effort. In the effort, we demonstrated the ability of scatterometry to non-destructively measure the trench depth, with results agreeing with subsequent SEM measurements of the same samples to better than 2 nm.

## PUBLICATIONS ENABLED BY THIS EQUIPMENT GRANT

This Equipment Grant to a large degree enabled scatterometer research results that lead to 8 refereed journal publications and 15 non-refereed publications (conference proceedings). The most recent refereed journal publications are attached.

# Scatterometry measurement of sub-0.1 $\mu$m linewidth gratings

Stephen A. Coulombe,[a] Babar K. Minhas, and Christopher J. Raymond
*University of New Mexico, Center for High Technology Materials, 1313 Goddard S.E., Albuquerque, New Mexico 87106*

S. Sohail H. Naqvi
*GIK Institute of Engineering Science and Technology, Topi, Pakistan*

John R. McNeil
*University of New Mexico, Center for High Technology Materials, 1313 Goddard S.E., Albuquerque, New Mexico 87106*

(Received 7 August 1997; accepted 21 November 1997)

The effort discussed here addresses the use of shorter incident wavelengths for characterizing sub-0.1 $\mu$m linewidths and the corresponding influence on scatterometry measurement sensitivity to linewidth variations. A sensitivity metric, based on the variance statistic, was developed using well-characterized, large-pitch (0.80 $\mu$m) photoresist grating structures on Si illuminated at 633 and 442 nm. The same metric was applied to short-pitch (0.20 $\mu$m), etched gratings on InP, with the result that appreciable scatterometry sensitivity was measured, even at the 633 nm incident wavelength. Modeling was used to estimate scatterometry sensitivity at three wavelengths for photoresist critical dimensions of 100 and 70 nm on Si. A significant increase in sensitivity was not found until the incident wavelength was reduced to 325 nm. We are presently investigating techniques to improve measurement sensitivity for short-pitch structures using the 633 nm incident wavelength. © *1998 American Vacuum Society.* [S0734-211X(98)08101-3]

## I. INTRODUCTION

Diffraction has long been used to measure linewidths of grating test structures, evolving into the metrology technique called scatterometry.[1–3] The use of scatterometry for semiconductor metrology has been widely reported.[4–10] Optical scatterometric techniques have been developed and refined for measuring grating test structures on substrate materials, primarily for semiconductor manufacturing applications. With the same lithographic, etch, and subsequent processing steps used for a device's critical dimensions (CD)—for example, transistor gates—the test structure, coupled with scatterometry measurements, allows improved monitoring, and potentially control, of device processing. Using optical scatterometry, it is possible to implement in-line and in some applications *in situ* metrology to support device processing, key elements identified in the *National Technology Roadmap for Semiconductors* for both lithographic and interconnect processes.[11]

The Technology Roadmap projects that in order to meet sub-0.1 $\mu$m CD requirements, processing tolerances of tens of nanometers, and metrology capabilities one tenth of that, or ~1 nm, will be necessary. There also will be a trend for uniformity measurements on the wafer to increase from a few points (~CY1994) to wafer map (~CY2001) to intrachip (~CY2007). These needs drive the search for accurate, high-speed, repeatable, noncontact CD metrology tools. However, as CDs continue to shrink below 0.5 $\mu$m, the viability of current-technology metrology tools diminishes. Some have placed the limit of optical imaging metrology, i.e., optical microscopy, in the range of 0.5–0.8 $\mu$m.[12]

To assess linewidth metrology well below 0.5 $\mu$m using scatterometry, we have performed measurements of etched gratings with linewidths less than 0.1 $\mu$m, and we believe this optical technique has considerable potential as a metrology tool, even at these very small linewidths. Scatterometry is not an optical imaging technique; it involves measurement and analysis of the diffracted coherent illumination of a sample. The constraining physical process for optical imaging, that is, diffraction, is applied to advantage as the very basis of scatterometry. As a consequence of the phase information present in diffraction signatures, scatterometry may achieve high measurement precision of lines much smaller than the incident light wavelength. However, this requires measuring a number of lines at once, determined by the size of the incident laser spot, which in our experiments was 100–200 $\mu$m. The result is an average linewidth value which is less susceptible to small line-to-line variations which would more seriously impact a single scanning electron microscopy (SEM) measurement. The scatterometry technique, because of this averaging, may be somewhat insensitive to small-scale, single or localized defects, that is, defects on a scale of a few $\mu$m or below. We have been able to detect grating uniformity variations over large, ~ mm to ~ cm, areas of the Si wafer; however, discussion of these uniformity measurements is beyond the scope of this article. Because standards for sub-0.5 $\mu$m dimensions are nonexistent, assessment of metrology options is difficult.[13] However, considering the attributes of scatterometry, i.e., noncontact, nondestructive, accurate, sensitive, repeatable, with simultaneous multilayer film measurement capabilities, it is of interest to explore the limits of scatterometry for deep submicron (~0.1 $\mu$m) linewidths.

---

[a] Electronic mail: coulombs@chtm.unm.edu

0734-211X/98/16(1)/80/8/$10.00 ©1998 American Vacuum Society

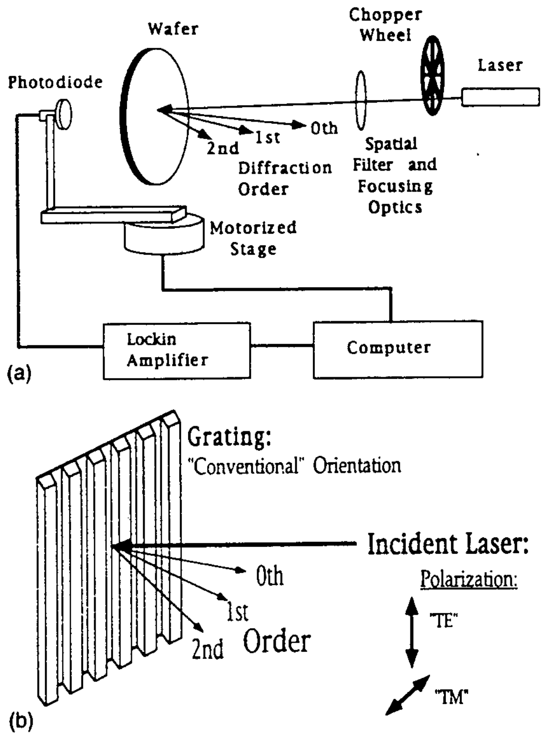

FIG. 1. (a) 2-Θ scatterometer experimental arrangement (b) configurations: conventional orientation, TE or TM.

Much of the recently reported work in scatterometric metrology has been applied to contemporary process technology (0.25–0.5 μm linewidths) using semiconductor samples for the experimental verification of modeling efforts.[8,14,15] For these developed photoresist CDs, grating pitches (periods) of 0.75–1.0 μm have been used. Simulations of 0.07 and 0.1 μm CD structures generally showed less distinction in the character of the scatterometry "signatures" and less variation of those signatures with CD changes, i.e., less sensitivity. Yoon *et al.* and Minhas *et al.* have speculated that using shorter wavelengths might recover the sensitivity that appears to be lost in application of scatterometry to small CDs.[16,17] We report here the results of using a shorter operating wavelength (442 nm) in a laboratory scatterometer. In addition, we have applied computer analyses using rigorous coupled wave theory (RCWT[18]) to assess sensitivity at 325 nm incident wavelength using scatterometry.

## II. EXPERIMENTAL ARRANGEMENT

The experimental arrangement is illustrated in Fig. 1. The sample wafer containing the test grating(s) was mounted on computer-controlled rotation and translation stages. The photodiode detector, also under computer control, could be rotated completely around the sample. The intensity of a diffracted order of the laser beam reflected from the grating was "tracked" by the detector, which measures the intensity as the angle of incidence (Θ) is changed. The result was a distinctive signature which depends on the grating's dimensions, underlying film thicknesses, and the refractive indices of the grating and films. We have chosen to analyze a developed photoresist line pattern (grating) on an anti-reflective coating (ARC) over Si. This photoresist grating has been fabricated at the University of New Mexico's Center for High Technology Materials, with well-defined geometric characteristics of pitch ~0.3–0.4 μm, linewidth ~0.12 μm, and vertical sidewalls. It is straightforward to analyze other materials, geometries, and underlying film layers with the scatterometry technique, as is done in a number of the references. The basis for the analysis of scatterometry experimental data is building a representative computer-based model of the grating, to include the complex indices of refraction for each component material, a geometric "shape" profile of the grating, and thickness of each layer down to the substrate. Metallic coatings may be included as well. All of these parameters may be varied within the modeling process, knowing the nominal design and semiconductor processing ranges of variation, in order to calculate theoretical scatter signatures with which to match the experimental data. More detailed discussions of this experimental arrangement are contained in Refs. 8, 9, and 14.

In the sections which follow, reference is made to specific grating and laser polarization orientations. Four combinations were used: grating lines oriented either vertically ("conventional") or horizontally ("conical"); and laser beam polarization oriented either perpendicular ("TE") or parallel ("TM") to the plane of incidence. The plane of incidence is defined by the input laser beam vector and the vector normal to the sample, which is horizontal in Fig. 1.

## III. SCATTEROMETRY ACCURACY AND SENSITIVITY

### A. Preliminary experiments

Both sensitivity and accuracy are desirable characteristics of a metrology tool. As previously mentioned, the lack of a metrology standard for sub-0.5 μm linewidths complicates the assessment of metrology tool accuracy. In this article, analysis and comparison of scatterometry accuracy with other means such as SEM and atomic force microscopy (AFM) are not the primary goal; these have been treated in prior work.[8,9] For example, Raymond *et al.* have shown that top-down SEM measurements consistently exhibit a significant offset (bias) to scatterometric measurements, while scatterometry and cross-section SEM results agree quite well.

More recently we have characterized photoresist gratings on an ARC layer on Si, of nominal 0.25 and 0.35 μm linewidth and 0.75 and 0.8 μm pitch, respectively, and etched InP gratings of sub-0.1 μm linewidth and 0.2 μm pitch, using both 442 and 633 nm incident wavelengths. These larger-linewidth Si samples, because they were uniform and well characterized, first were used to develop a sensitivity metric. The availability of finer-linewidth InP samples allowed a collection of actual short-pitch data and a comparison with theory. These techniques were then applied theoretically to short-pitch, ~0.1 μm linewidth Si cases.

A sense of the correlation between the Si sample measurement results using the two incident wavelengths, along with SEM measurements, is possible by examining Fig. 2,

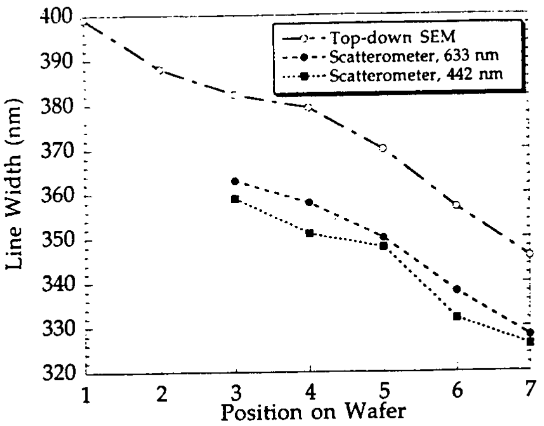

FIG. 2. Scatterometry linewidth measurements, TE conventional, at 633 and 442 nm compared to top-down SEM measurements for nominal 0.35 μm linewidth, 0.8 μm pitch photoresist-on-Si gratings.

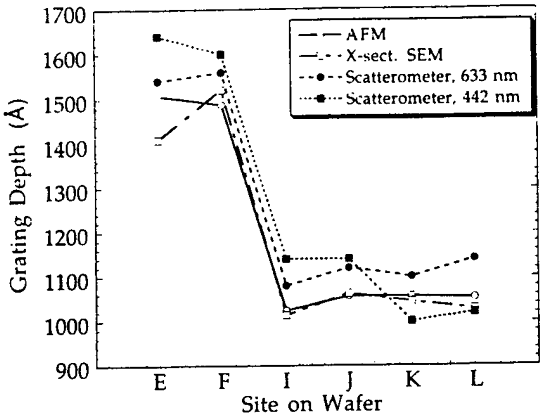

FIG. 4. Scatterometry depth measurements, TM conventional, at 633 and 442 nm compared to AFM and cross-section SEM measurements for sub-0.2 μm depth, 0.2 μm pitch InP etched gratings.

which compares the top-down SEM linewidth measurements to scatterometer measurements. A bias of approximately 20 nm can be seen. This bias has been observed previously in characterizing samples having similar structure, as noted above for results presented in Ref. 9. The current scatterometer measurements were determined with a computational resolution of 1 nm. The average linewidth difference between the 633 and 442 nm results is 4.2 nm, and both sets of these scatterometer data are correlated with the SEM data.

Results from characterizing the InP etched gratings having sub-0.1 μm linewidths are shown in Fig. 3. Six sites on an InP wafer were measured using the scatterometer at 633 and 442 nm incident wavelengths. The scatterometry data track the AFM results well: the average bias between the AFM measurements was 2.9 nm at the 633 nm wavelength and 3.8 nm at the 442 nm wavelength. The bias with the cross-section SEM data was greater: the average difference from SEM measurements was 9.1 nm at the 633 nm wavelength and 11.0 nm at the 442 nm wavelength. Note that the SEM measurements were taken at the same nominal scatterometry measurement sites. For the same InP samples, Fig. 4 shows measurements of grating depth. The scatterometry data are consistent with the AFM and SEM results: the average difference from AFM measurements was $-6.0$ nm at both wavelengths, and the offset from the cross-section SEM data was $-7.7$ nm at both wavelengths. It can be seen that all three techniques follow the same trends in linewidth and depth. These data demonstrate the potential of scatterometry for sub-0.1 μm linewidth metrology.

The sensitivity of scatterometry, i.e., how much the signatures change when a sample parameter is varied, is an important characteristic and ultimately determines linewidth measurement precision. While sensitivity might involve grating linewidth, depth, pitch, or underlying film thicknesses, our primary interest has been in the sensitivity to linewidth variation. In the following sections we focus on the sensitivity of scatterometry with respect to reduction in the operating wavelength.

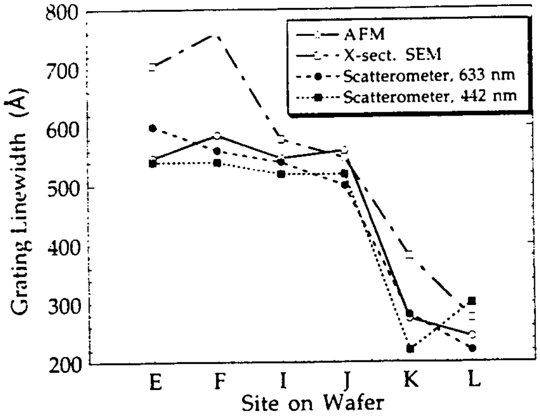

FIG. 3. Scatterometry linewidth measurements, TM conventional, at 633 and 442 nm compared to AFM and cross-section SEM measurements for sub-0.1 μm linewidth, 0.2 μm pitch InP etched gratings.

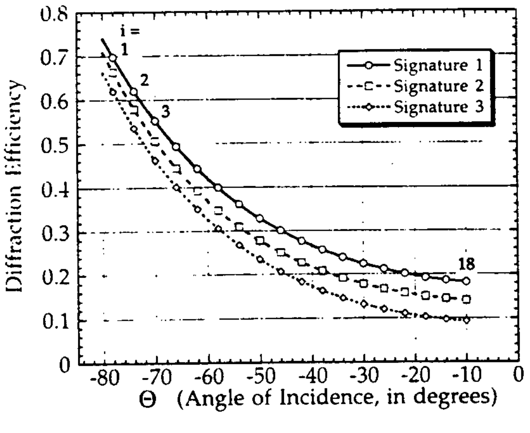

FIG. 5. Example scatterometry signatures for computation of avg. variance metric.

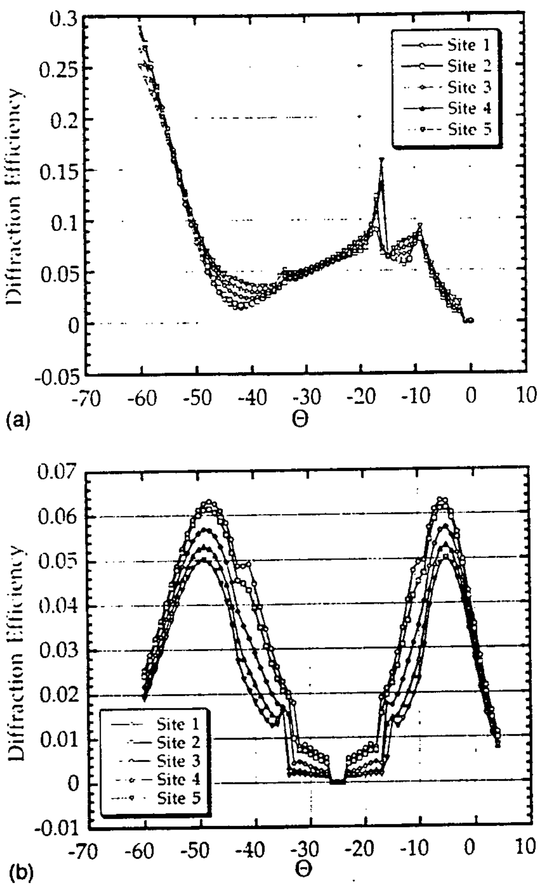

FIG. 6. Scatterometry measurements, TE conventional, at 633 nm of nominal 0.25 μm linewidth, 0.75 μm pitch photoresist-on-Si gratings, ~6 nm average linewidth increment between signatures, for (a) 0 order, (b) 1st order.

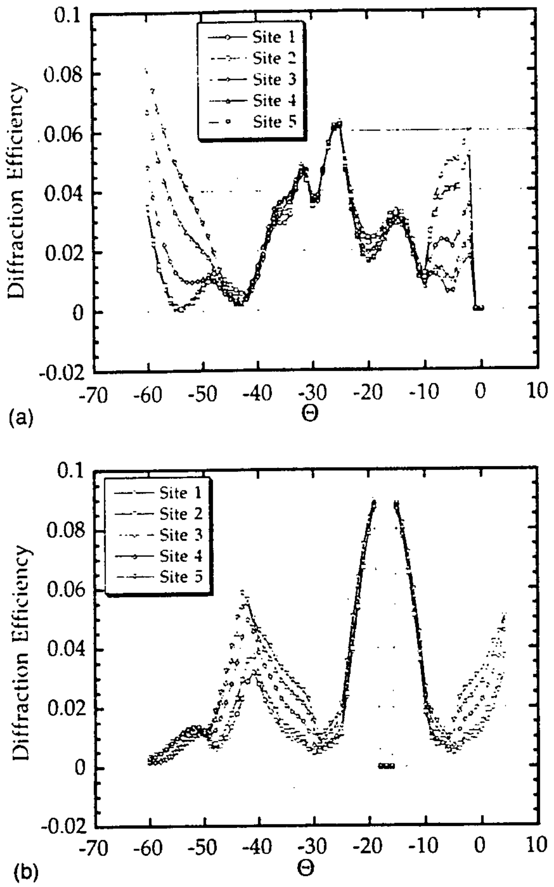

FIG. 7. Scatterometry measurements, TE conventional, at 442 nm of nominal 0.25 μm linewidth, 0.75 μm pitch photoresist-on-Si gratings, ~6 nm linewidth increment between signatures, for (a) 0 order, (b) 1st order.

### B. Sensitivity metric

In order to assess the sensitivity of the scatterometry technique at different wavelengths and for different samples, a common metric is required. We define sensitivity as the change in a measured parameter versus a change in a sample feature (e.g., linewidth). In scatterometry, the measured parameter is a point in the "scatterometer signature," which is a normalized intensity profile measured as a function of the angle of incidence of the laser beam to the sample. Hence these signatures represent a collection of many data points which characterize the change in diffraction efficiency of the sample as the angle of incidence of the illuminating laser is changed.

Quantitative, statistical measures of the overall signature change—or amount of spread between signatures corresponding to two samples having different linewidths—include range, mean absolute variation, variance, standard deviation, and mean-square error (MSE). Previously, we have used normalized MSE, an adaptation of our earlier (non-normalized) MSE computations for matching experimental data to model predictions when the two data sets are similar in range. However, the normalized MSE technique overemphasizes portions of the signature that have very small values of diffraction efficiency. A metric is desired that weights the entire signature evenly, as it is generally not known *a priori* what the shape of the experimental signature will be. To this end, we have chosen to use the average variance as the sensitivity metric, defined as

$$\overline{s^2}=\frac{1}{M}\sum_{i=1}^{M}\left[\frac{\sum_{j=1}^{n}(x_{ij}-\bar{x}_i)^2}{n-1}\right], \qquad (1)$$

where the term in brackets is recognized as the variance.[19] This term is computed by using the values of all signatures resulting from linewidth variations, i.e., $x_{ij}$ represents a diffraction efficiency for the $i$th incidence angle and the $j$th linewidth. The term preceding the brackets takes the average over all angles of incidence. This process is illustrated in Fig. 5 for three example signatures: at each angle of incidence, i.e., for $i=1,2,3...18$, the mean, $\bar{x}_i$, and a variance are computed. In this example, the number of signatures ($n$) is equal to 3, and the number of incident angles ($M$) is 18. The "average variance" is taken to be a measure of the spread between the curves, and in the following sections is referred to as "avg. variance". An average is appropriate as long as the CD increment is small, and changes are comparable in magnitude from one signature to the next. A larger value of avg. variance indicates higher measurement sensitivity, which is of value in a process metrology tool for nanometer-

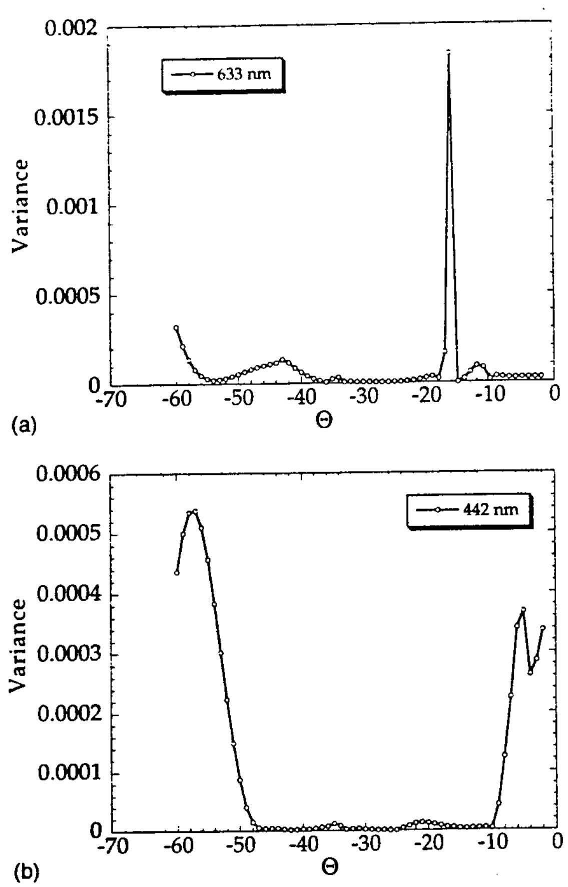

FIG. 8. Variance between signatures as a function of angle of incidence for 0-order scatterometry measurements. TE conventional, of nominal 0.25 $\mu$m linewidth, 0.75 $\mu$m pitch photoresist-on-Si gratings, ~6 nm linewidth increment between signatures, at (a) 633 nm, (b) 442 nm.

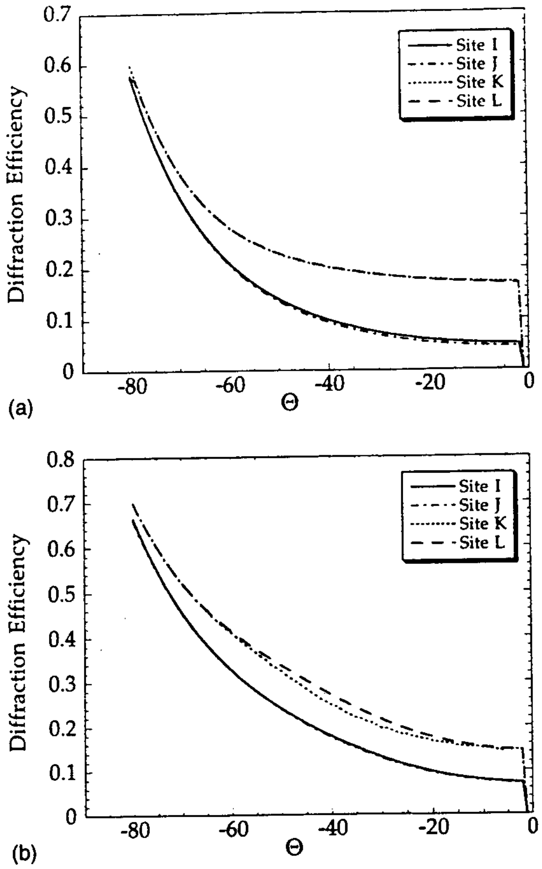

FIG. 9. Scatterometry measurements, TM conventional, of sub-0.1 $\mu$m linewidth, 0.2 $\mu$m pitch InP etched gratings, ~25 nm linewidth increment between *I*-*J* and *K*-*L* signatures, at (a) 633 nm, (b) 442 nm.

scale variations. Scatterometer signatures may exhibit considerably more structure than is shown in the example, as will be seen in the following sections.

## IV. WAVELENGTH EFFECTS ON MEASUREMENT SENSITIVITY

### A. Large-pitch samples

Initial experiments using 633 and 442 nm incident wavelengths were performed on samples obtained from SEMATECH. The samples consisted of developed photoresist patterns of nominal 0.35 $\mu$m lines, 0.80 $\mu$m pitch, and nominal 0.25 $\mu$m lines, 0.75 $\mu$m pitch. Samples with similar grating dimensions, along with conventional 633 nm scatterometer measurements, are described in detail by Raymond *et al.*[9]

Our task with this same type of grating structure was to determine whether the sensitivity of scatterometry was significantly improved by using shorter laser wavelengths. Because the pitch of these sample gratings was relatively large with respect to the operating wavelengths, both 0- and 1st-order diffraction were characterized. A typical series of measurements is shown in Figs. 6(a) and 6(b) and 7(a) and 7(b) for 633 and 442 nm laser wavelengths, respectively. Stepping from test site to test site corresponds to a linewidth increment of nominally 6 nm. The following trends can be observed from the signatures. When the pitch is large compared to the incident wavelength, as in the current example, the 1st order may show more sensitivity than the 0 order. For example, where sensitivity appears low for 633 nm in the 0-order signature [Fig. 6(a)], it is recovered in the 1st-order signatures [Fig. 6(b)]. At 442 nm, there is sensitivity in the 0 order [Fig. 7(a)] as well as in 1st-order [Fig. 7(b)] signatures. Also, it can be observed that at 442 nm there is more "structure" to the signatures, which helps to differentiate between CD increments. There is a noticeable spreading between the signatures, and this occurs at different angular locations depending upon diffraction order, wavelength, mounting configuration, and laser polarization. Applying the avg. variance sensitivity metric to the 0-order data, the resulting values are $7.95\times10^{-5}$ for 633 nm and $1.07\times10^{-4}$ for 442 nm, indicating a 35% sensitivity improvement at 442 nm. The individual variances used to compute the avg. variance are plotted in Figs. 8(a) and 8(b) as a function of incidence angle, Θ. These variance plots are helpful in identifying regions of maximum sensitivity as the angle of incidence is varied, again depending upon the sample and measurement details. For example, Fig. 8(a) shows a narrow region of higher sensitivity near 16° angle of incidence, while sensitivity is low at all other angles. At 442 nm, as shown in Fig. 8(b), two broader regions of sensitivity are indicated, from 2° to 8° and

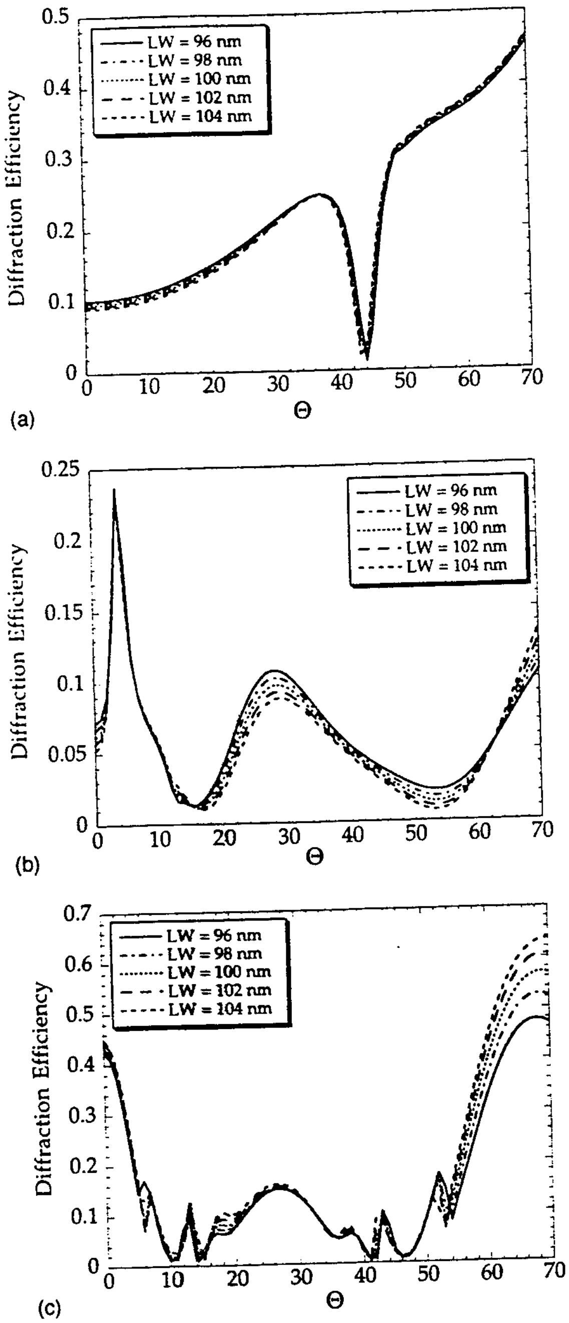

FIG. 10. Scatterometry model results, TE conventional, for nominal 0.1 $\mu$m linewidth, 0.36 $\mu$m pitch photoresist-on-ARC-on-Si gratings, 2 nm linewidth increment between signatures, at (a) 633 nm, (b) 442 nm, (c) 325 nm.

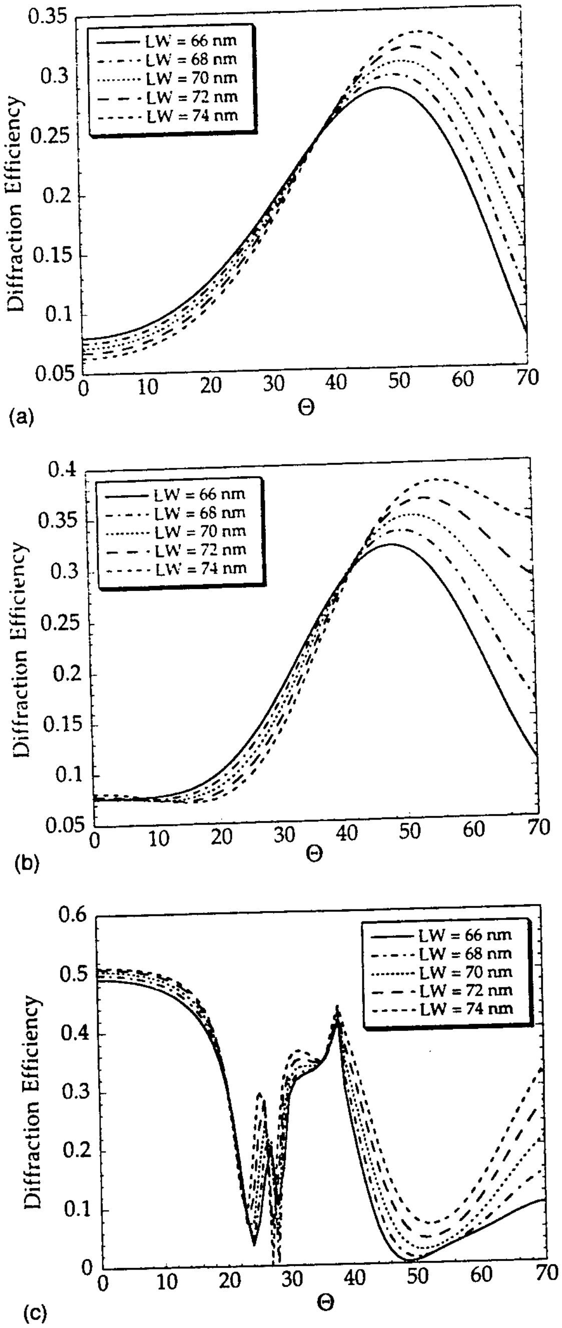

FIG. 11. Scatterometry model results, TE conventional, for nominal 0.07 $\mu$m linewidth, 0.2 $\mu$m pitch photoresist-on-ARC-on-Si gratings, 2 nm linewidth increment between signatures, at (a) 633 nm, (b) 442 nm, (c) 325 nm.

above 50°. These observations are consistent with the subjective assessment of signature "spreading" as linewidth is varied, as discussed in connection with Figs. 6(a) and 7(a). Having developed and tested a sensitivity metric, it was desired to investigate shorter-pitch grating samples with sub-0.1 $\mu$m linewidths.

## B. Short-pitch samples

The samples of etched InP gratings previously mentioned in connection with Figs. 3 and 4 were used for this investigation. Although not representative of Si technology in terms of material or dimensions, these were the only uniform, well-characterized sub-0.1 $\mu$m CD samples available. The nominal grating pitch was 0.2 $\mu$m, with linewidths ranging from 25 to 55 nm, and depths of 100 to 200 nm. Because this pitch is considerably smaller than the incident wavelength, the grating only produces 0-order diffraction at 633 and 442 nm wavelengths. Scatterometer signatures for the TM-conventional mounting mode are shown in Figs. 9(a) and 9(b) for the two wavelengths, respectively. A computation resolution of 2 nm was used, and the nominal CD increment on the wafer was 25 nm in this case. The avg. variances for

TABLE I. Summary of avg. variances for all configurations vs $\lambda_0$, for 100 nm lines.

| $\lambda_0$ | Conventional | | Conic | |
|---|---|---|---|---|
| (nm) | TE | TM | TE | TM |
| 633 | 4.3e−5 | 1.0e−5 | 4.5e−5 | 9.8e−6 |
| 442 | 3.0e−5 | 1.0e−5 | 4.4e−5 | 3.0e−5 |
| 325 | 7.0e−4 | 7.1e−4 | 1.6e−3 | 2.7e−4 |

TABLE II. Summary of avg. variances for all configurations vs $\lambda_0$, for 70 nm lines.

| $\lambda_0$ | Conventional | | Conic | |
|---|---|---|---|---|
| (nm) | TE | TM | TE | TM |
| 633 | 5.1e−4 | 2.4e−6 | 1.3e−4 | 3.5e−5 |
| 442 | 1.1e−3 | 2.0e−5 | 7.7e−5 | 2.5e−5 |
| 325 | 1.6e−3 | 6.9e−4 | 4.1e−4 | 2.0e−4 |

these signatures are $4.40\times10^{-3}$ at 633 nm and $2.47\times10^{-3}$ at 442 nm, showing no significant influence on the sensitivity by using the shorter measurement wavelength. Note, however, that scatterometry, even at the 633 nm incident wavelength, exhibits sufficient sensitivity to remain a useful tool for detecting changes in linewidth in the 0.05 $\mu$m CD region.

Overall sensitivity can be compared to those levels reported above for large-pitch samples by dividing the large- and short-pitch avg. variance metrics by the respective linewidth increments in each case, yielding a variance-per-nm figure. At 633 nm wavelength, the result is $1.3\times10^{-5}$ nm$^{-1}$ for the large-pitch sample and $1.8\times10^{-4}$ nm$^{-1}$ for the short-pitch sample. At 442 nm, the result is $1.8\times10^{-5}$ nm$^{-1}$ for the large-pitch sample and $9.9\times10^{-5}$ nm$^{-1}$ for the short-pitch sample. At both wavelengths, somewhat greater sensitivity per nm was observed with the short-pitch sample. Such a result is surprising if one considers that as the linewidth and pitch of the grating are reduced below the incident wavelength, $\lambda_0$, these features have less and less effect and begin to approximate a surface roughness on a scale $\ll\lambda_0$. This result quite possibly is due to the dissimilar materials and dimensions between the photoresist-on-Si and the etched InP samples and suggests that other factors, in addition to wavelength, also influence sensitivity. Hence, we do not regard the differences in sensitivity shown with these dissimilar samples to be noteworthy. Experimentally, we have observed that the structure, or variation, within diffraction signatures tends to disappear as the pitch and linewidth are reduced. Note the Fresnel-like characteristics of the short-pitch InP samples in Fig. 9(a), as compared to the less-predictably varying large-pitch signatures in Fig. 6(a). In Fig. 10, one observes that the signatures contain more structure as the incident wavelength is reduced.

## C. Modeling of sub-0.1 $\mu$m photoresist-on-silicon gratings

To assess the measurement sensitivity for a short-pitch photoresist structure with dimensions consistent with Technology Roadmap projections, the diffraction of nominal 70 and 100 nm linewidth photoresist grating structures on Si was investigated using computer modeling: well-characterized samples were not available for actual measurements. The grating pitches were fixed at 0.20 and 0.36 $\mu$m, respectively. Resist height was 0.5 $\mu$m, and an anti-reflection layer (ARC) of 75 nm was included between the resist and the Si substrate. Diffraction from these structures was evaluated at laser wavelengths of 633, 442, and 325 nm, and the refractive indices for resist, ARC and Si, were set corresponding to each wavelength. Five linewidth steps in increments of 2 nm were modeled at each wavelength: nominal linewidth, nominal ±2 nm, and nominal ±4 nm.

A representative set of signatures, in this case for the TE-conventional measurement configuration, are shown in Figs. 10(a)–10(c) and 11(a)–11(c) for the nominal 100 and 70 nm linewidths, respectively. Tables I and II summarize the sensitivity metric data for the 100 and 70 nm cases, respectively, for the four combinations of TE/TM input polarization and conventional/conical grating mounting.

These avg. variance data are plotted in Figs. 12(a) and 12(b). Qualitatively, it can be observed in Figs. 10 and 11 that the spreading between signatures increases for decreasing incident wavelength. The metric plots of Fig. 12 indicate, however, that the benefit in sensitivity is not pronounced

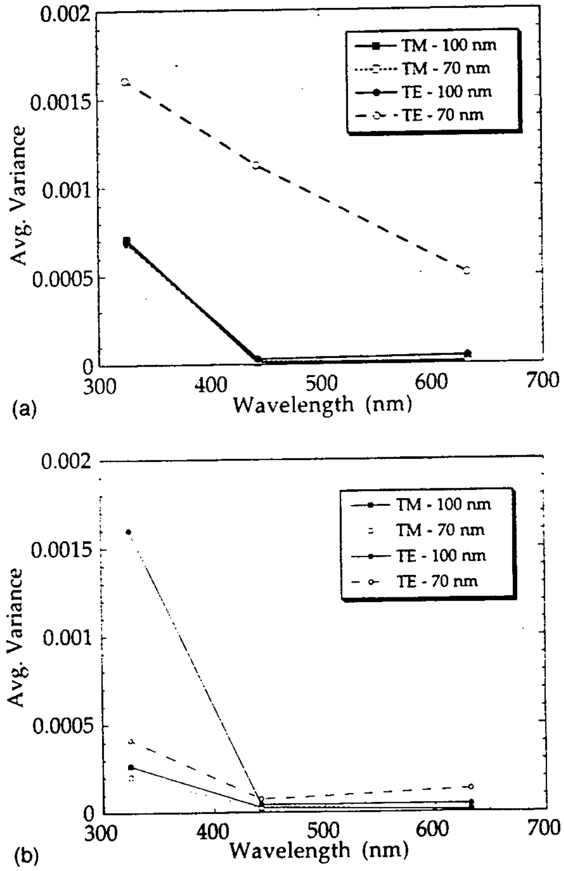

FIG. 12. Avg. variance as a function of wavelength from scatterometry model results, for nominal 0.07 and 0.1 $\mu$m linewidths, photoresist-on-ARC-on-Si gratings, for (a) TE and TM conventional, (b) TE and TM conic.

until the wavelength is reduced to 325 nm. An exception to this trend is observed for the TE-conventional case for nominal 70 nm linewidths, as shown in Fig. 12(a). The increase in sensitivity for this particular configuration may be related to the pitch of the grating and is an area requiring further investigation. The implication is that there may be ways of increasing the scatterometry measurement sensitivity by careful selection of test grating dimensions. Prefabrication modeling would allow an optimum test structure to be designed.

## V. CONCLUSIONS

In response to the need to assess measurement sensitivity, an avg. variance metric was developed. This metric was then used to compare scatterometer measurement sensitivity at multiple wavelengths, to determine angular regions of sensitivity, and to gain insight into the influence of other parameters on measurement sensitivity.

When the pitch of the sample is large compared to the incident wavelength, the 1st order may be useful, i.e., where sensitivity is low for the 0-order signature, it possibly may be recovered in the 1st order. At 442 nm there was still significant sensitivity at 0 order and at 1st order, and there was more structure to the signatures, which helps to differentiate between CD increments. For shorter-pitch structures for which only a 0-order diffraction signature is possible, structure in the signature is reduced, but the signature still exhibits its sensitivity to linewidth variations when using the 633 nm incident wavelength.

From these data, it can be concluded that the strategy of reducing the scatterometer operating wavelength may increase sensitivity significantly, particularly at the 325 nm wavelength. However, such an improvement is quite dependent on the sample materials involved and the grating test structure. For photoresist grating structures on Si, it appears that scatterometry measurement sensitivity can be positively influenced by judicious selection of test structure dimensions. We are presently investigating additional techniques for increasing measurement sensitivity for sub-0.1 μm structures while maintaining use of the convenient 633 nm laser wavelength.

## ACKNOWLEDGMENTS

Wafer samples and SEM/AFM measurements used in these studies were provided by SEMATECH and Lucent Technologies. The authors thank SRC and ARPA for partial financial support of this work.

[1] H. P. Kleinknecht and H. Meier, J. Electrochem. Soc. **125**, 798 (1978).

[2] H. P. Kleinknecht and H. Meier, Appl. Opt. **19**, 525 (1980).

[3] M. G. Moharam and T. K. Gaylord, J. Opt. Soc. Am. **72**, 1385 (1982).

[4] J. R. McNeil, S. S. H. Naqvi, S. M. Gaspar, K. C. Hickman, K. P. Bishop, L. M. Milner, R. H. Krukar, and G. A. Petersen, Microlithography World **1**, 16 (1992).

[5] S. S. H. Naqvi, J. R. McNeil, R. H. Krukar, and K. P. Bishop, Microlithography World **2**, 5 (1993).

[6] R. H. Krukar, S. L. Prins, D. M. Krukar, G. A. Petersen, S. M. Gaspar, J. R. McNeil, S. S. H. Naqvi, and D. R. Hush, Proc. SPIE **1926**, 60 (1993).

[7] M. R. Murnane, C. J. Raymond, S. S. H. Naqvi, and J. R. McNeil, Proc. SPIE **2532**, 251 (1995).

[8] C. J. Raymond, M. R. Murnane, S. S. H. Naqvi, and J. R. McNeil, J. Vac. Sci. Technol. B **13**, 1484 (1995).

[9] C. J. Raymond, M. R. Murnane, S. L. Prins, S. S. H. Naqvi, and J. R. McNeil, J. Vac. Sci. Technol. B **15**, 361 (1997).

[10] J. Bishoff, J. W. Baumgart, and H. Truckenbrodt, Proc. SPIE **2725**, 678 (1996).

[11] *The National Technology Roadmap for Semiconductors* (Semiconductor Industry Association, San Jose, 1994).

[12] R. Iscoff, Semicond. Int. **17**, 56 (1994).

[13] D. Nyyssonen and R. D. Larrabee, NBS J. Res. **92**, 187 (1987).

[14] C. J. Raymond, J. R. McNeil, and S. S. H. Naqvi, Proc. SPIE **2725**, 720 (1996).

[15] S. L. Prins, L. M. Milner, S. H. Zaidi, S. S. H. Naqvi, and J. R. McNeil, SRC TECHON 93 Extended Abstracts 447 (1993).

[16] E. Yoon, C. A. Green, R. A. Gottscho, T. R. Hayes, and K. P. Giapis, J. Vac. Sci. Technol. B **10**, 2230 (1992).

[17] B. Minhas, S. L. Prins, S. S. H. Naqvi, and J. R. McNeil, Proc. SPIE **2725**, 729 (1996).

[18] T. K. Gaylord and M. G. Moharram, Proc. IEEE **73**, 894 (1985).

[19] M. Hamburg, *Statistical Analysis for Decision Making* (Harcourt Brace Jovanovich, New York, 1977), p. 39.

# Scatterometry measurement of sub-0.1 $\mu$m linewidth gratings

Stephen A. Coulombe,[a] Babar K. Minhas, and Christopher J. Raymond
*University of New Mexico, Center for High Technology Materials, 1313 Goddard S.E., Albuquerque, New Mexico 87106*

S. Sohail H. Naqvi
*GIK Institute of Engineering Science and Technology, Topi, Pakistan*

John R. McNeil
*University of New Mexico, Center for High Technology Materials, 1313 Goddard S.E., Albuquerque, New Mexico 87106*

(Received 7 August 1997; accepted 21 November 1997)

The effort discussed here addresses the use of shorter incident wavelengths for characterizing sub-0.1 $\mu$m linewidths and the corresponding influence on scatterometry measurement sensitivity to linewidth variations. A sensitivity metric, based on the variance statistic, was developed using well-characterized, large-pitch (0.80 $\mu$m) photoresist grating structures on Si illuminated at 633 and 442 nm. The same metric was applied to short-pitch (0.20 $\mu$m), etched gratings on InP, with the result that appreciable scatterometry sensitivity was measured, even at the 633 nm incident wavelength. Modeling was used to estimate scatterometry sensitivity at three wavelengths for photoresist critical dimensions of 100 and 70 nm on Si. A significant increase in sensitivity was not found until the incident wavelength was reduced to 325 nm. We are presently investigating techniques to improve measurement sensitivity for short-pitch structures using the 633 nm incident wavelength. © *1998 American Vacuum Society.* [S0734-211X(98)08101-3]

## I. INTRODUCTION

Diffraction has long been used to measure linewidths of grating test structures, evolving into the metrology technique called scatterometry.[1-3] The use of scatterometry for semiconductor metrology has been widely reported.[4-10] Optical scatterometric techniques have been developed and refined for measuring grating test structures on substrate materials, primarily for semiconductor manufacturing applications. With the same lithographic, etch, and subsequent processing steps used for a device's critical dimensions (CD)—for example, transistor gates—the test structure, coupled with scatterometry measurements, allows improved monitoring, and potentially control, of device processing. Using optical scatterometry, it is possible to implement in-line and in some applications *in situ* metrology to support device processing, key elements identified in the *National Technology Roadmap for Semiconductors* for both lithographic and interconnect processes.[11]

The Technology Roadmap projects that in order to meet sub-0.1 $\mu$m CD requirements, processing tolerances of tens of nanometers, and metrology capabilities one tenth of that, or ~1 nm, will be necessary. There also will be a trend for uniformity measurements on the wafer to increase from a few points (~CY1994) to wafer map (~CY2001) to intrachip (~CY2007). These needs drive the search for accurate, high-speed, repeatable, noncontact CD metrology tools. However, as CDs continue to shrink below 0.5 $\mu$m, the viability of current-technology metrology tools diminishes. Some have placed the limit of optical imaging metrology, i.e., optical microscopy, in the range of 0.5–0.8 $\mu$m.[12]

To assess linewidth metrology well below 0.5 $\mu$m using scatterometry, we have performed measurements of etched gratings with linewidths less than 0.1 $\mu$m, and we believe this optical technique has considerable potential as a metrology tool, even at these very small linewidths. Scatterometry is not an optical imaging technique; it involves measurement and analysis of the diffracted coherent illumination of a sample. The constraining physical process for optical imaging, that is, diffraction, is applied to advantage as the very basis of scatterometry. As a consequence of the phase information present in diffraction signatures, scatterometry may achieve high measurement precision of lines much smaller than the incident light wavelength. However, this requires measuring a number of lines at once, determined by the size of the incident laser spot, which in our experiments was 100–200 $\mu$m. The result is an average linewidth value which is less susceptible to small line-to-line variations which would more seriously impact a single scanning electron microscopy (SEM) measurement. The scatterometry technique, because of this averaging, may be somewhat insensitive to small-scale, single or localized defects, that is, defects on a scale of a few $\mu$m or below. We have been able to detect grating uniformity variations over large, ~ mm to ~ cm, areas of the Si wafer; however, discussion of these uniformity measurements is beyond the scope of this article. Because standards for sub-0.5 $\mu$m dimensions are nonexistent, assessment of metrology options is difficult.[13] However, considering the attributes of scatterometry, i.e., noncontact, nondestructive, accurate, sensitive, repeatable, with simultaneous multilayer film measurement capabilities, it is of interest to explore the limits of scatterometry for deep submicron (~0.1 $\mu$m) linewidths.

---

[a] Electronic mail: coulombs@chtm.unm.edu

0734-211X/98/16(1)/80/8/$10.00 ©1998 American Vacuum Society

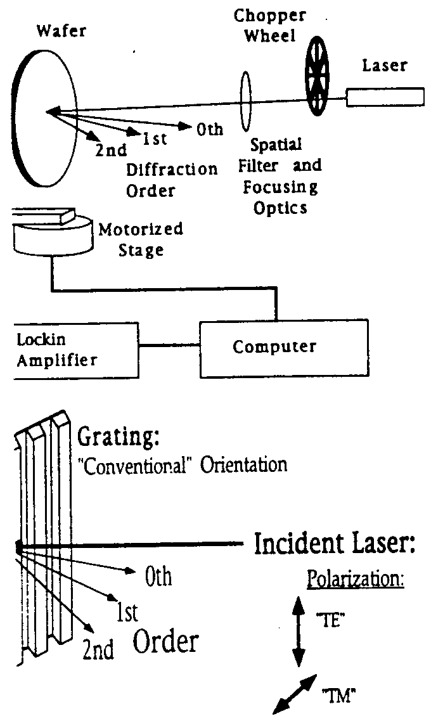

FIG. 1. erometer experimental arrangement (b) configurations:
convent ion, TE or TM.

Muc the recently reported work in scatterometric me-
trology been applied to contemporary process technology
(0.25– μm linewidths) using semiconductor samples for
the exp mental verification of modeling efforts.[8,14,15] For
these d oped photoresist CDs, grating pitches (periods) of
0.75– m have been used. Simulations of 0.07 and 0.1
μm C es generally showed less distinction in the
charac scatterometry "signatures" and less varia-
tion o natures with CD changes, i.e., less sensitiv-
ity. Y nd Minhas *et al.* have speculated that using
shorte gths might recover the sensitivity that ap-
pears in application of scatterometry to small
CDs. ort here the results of using a shorter oper-
ating (442 nm) in a laboratory scatterometer. In
additi e applied computer analyses using rigorous
couple eory (RCWT[18]) to assess sensitivity at 325
nm in elength using scatterometry.

## II. EX ITAL ARRANGEMENT

The ntal arrangement is illustrated in Fig. 1. The
sampl ntaining the test grating(s) was mounted on
comp lled rotation and translation stages. The pho-
todio also under computer control, could be ro-
tated around the sample. The intensity of a dif-
fract he laser beam reflected from the grating was
"track e detector, which measures the intensity as
the an dence (Θ) is changed. The result was a dis-
tinctiv e which depends on the grating's dimen-
sions, film thicknesses, and the refractive indices
of the d films. We have chosen to analyze a developed photoresist line pattern (grating) on an anti-reflective coating (ARC) over Si. This photoresist grating has been fabricated at the University of New Mexico's Center for High Technology Materials, with well-defined geometric characteristics of pitch ~0.3–0.4 μm, linewidth ~0.12 μm, and vertical sidewalls. It is straightforward to analyze other materials, geometries, and underlying film layers with the scatterometry technique, as is done in a number of the references. The basis for the analysis of scatterometry experimental data is building a representative computer-based model of the grating, to include the complex indices of refraction for each component material, a geometric "shape" profile of the grating, and thickness of each layer down to the substrate. Metallic coatings may be included as well. All of these parameters may be varied within the modeling process, knowing the nominal design and semiconductor processing ranges of variation, in order to calculate theoretical scatter signatures with which to match the experimental data. More detailed discussions of this experimental arrangement are contained in Refs. 8, 9, and 14.

In the sections which follow, reference is made to specific grating and laser polarization orientations. Four combinations were used: grating lines oriented either vertically ("conventional") or horizontally ("conical"); and laser beam polarization oriented either perpendicular ("TE") or parallel ("TM") to the plane of incidence. The plane of incidence is defined by the input laser beam vector and the vector normal to the sample, which is horizontal in Fig. 1.

## III. SCATTEROMETRY ACCURACY AND SENSITIVITY

### A. Preliminary experiments

Both sensitivity and accuracy are desirable characteristics of a metrology tool. As previously mentioned, the lack of a metrology standard for sub-0.5 μm linewidths complicates the assessment of metrology tool accuracy. In this article, analysis and comparison of scatterometry accuracy with other means such as SEM and atomic force microscopy (AFM) are not the primary goal; these have been treated in prior work.[8,9] For example, Raymond *et al.* have shown that top-down SEM measurements consistently exhibit a significant offset (bias) to scatterometric measurements, while scatterometry and cross-section SEM results agree quite well.

More recently we have characterized photoresist gratings on an ARC layer on Si, of nominal 0.25 and 0.35 μm linewidth and 0.75 and 0.8 μm pitch, respectively, and etched InP gratings of sub-0.1 μm linewidth and 0.2 μm pitch, using both 442 and 633 nm incident wavelengths. These larger-linewidth Si samples, because they were uniform and well characterized, first were used to develop a sensitivity metric. The availability of finer-linewidth InP samples allowed a collection of actual short-pitch data and a comparison with theory. These techniques were then applied theoretically to short-pitch, ~0.1 μm linewidth Si cases.

A sense of the correlation between the Si sample measurement results using the two incident wavelengths, along with SEM measurements, is possible by examining Fig. 2,

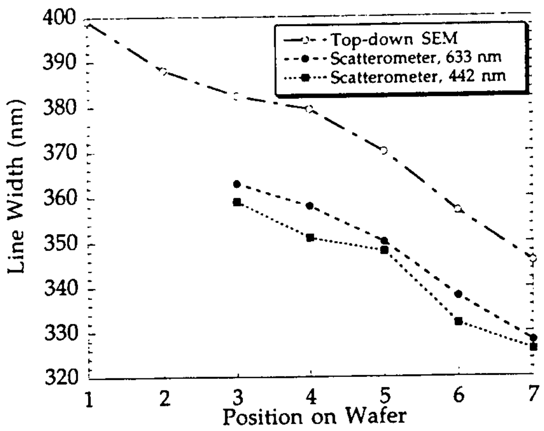

FIG. 2. Scatterometry linewidth measurements, TE conventional, at 633 and 442 nm compared to top-down SEM measurements for nominal 0.35 $\mu$m linewidth, 0.8 $\mu$m pitch photoresist-on-Si gratings.

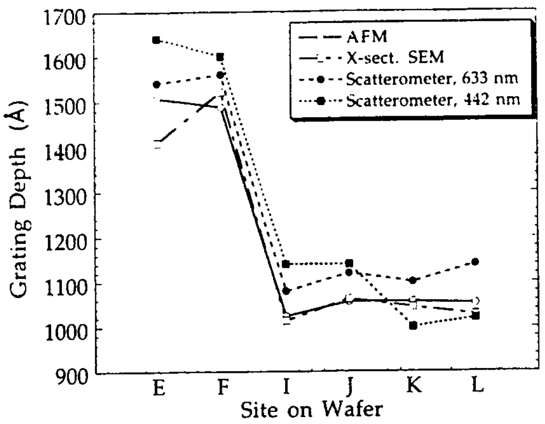

FIG. 4. Scatterometry depth measurements, TM conventional, at 633 and 442 nm compared to AFM and cross-section SEM measurements for sub-0.2 $\mu$m depth, 0.2 $\mu$m pitch InP etched gratings.

which compares the top-down SEM linewidth measurements to scatterometer measurements. A bias of approximately 20 nm can be seen. This bias has been observed previously in characterizing samples having similar structure, as noted above for results presented in Ref. 9. The current scatterometer measurements were determined with a computational resolution of 1 nm. The average linewidth difference between the 633 and 442 nm results is 4.2 nm, and both sets of these scatterometer data are correlated with the SEM data.

Results from characterizing the InP etched gratings having sub-0.1 $\mu$m linewidths are shown in Fig. 3. Six sites on an InP wafer were measured using the scatterometer at 633 and 442 nm incident wavelengths. The scatterometry data track the AFM results well: the average bias between the AFM measurements was 2.9 nm at the 633 nm wavelength and 3.8 nm at the 442 nm wavelength. The bias with the cross-section SEM data was greater: the average difference from SEM measurements was 9.1 nm at the 633 nm wavelength and 11.0 nm at the 442 nm wavelength. Note that the SEM measurements were taken at the same nominal scatterometry measurement sites. For the same InP samples, Fig. 4 shows measurements of grating depth. The scatterometry data are consistent with the AFM and SEM results: the average difference from AFM measurements was $-6.0$ nm at both wavelengths, and the offset from the cross-section SEM data was $-7.7$ nm at both wavelengths. It can be seen that all three techniques follow the same trends in linewidth and depth. These data demonstrate the potential of scatterometry for sub-0.1 $\mu$m linewidth metrology.

The sensitivity of scatterometry, i.e., how much the signatures change when a sample parameter is varied, is an important characteristic and ultimately determines linewidth measurement precision. While sensitivity might involve grating linewidth, depth, pitch, or underlying film thicknesses, our primary interest has been in the sensitivity to linewidth variation. In the following sections we focus on the sensitivity of scatterometry with respect to reduction in the operating wavelength.

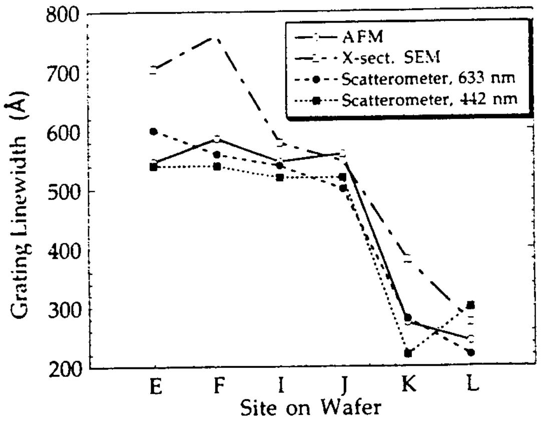

FIG. 3. Scatterometry linewidth measurements, TM conventional, at 633 and 442 nm compared to AFM and cross-section SEM measurements for sub-0.1 $\mu$m linewidth, 0.2 $\mu$m pitch InP etched gratings.

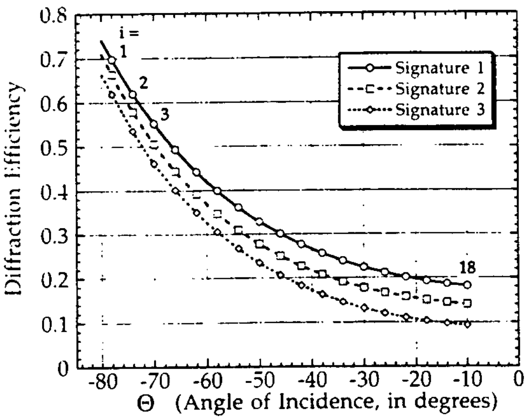

FIG. 5. Example scatterometry signatures for computation of avg. variance metric.

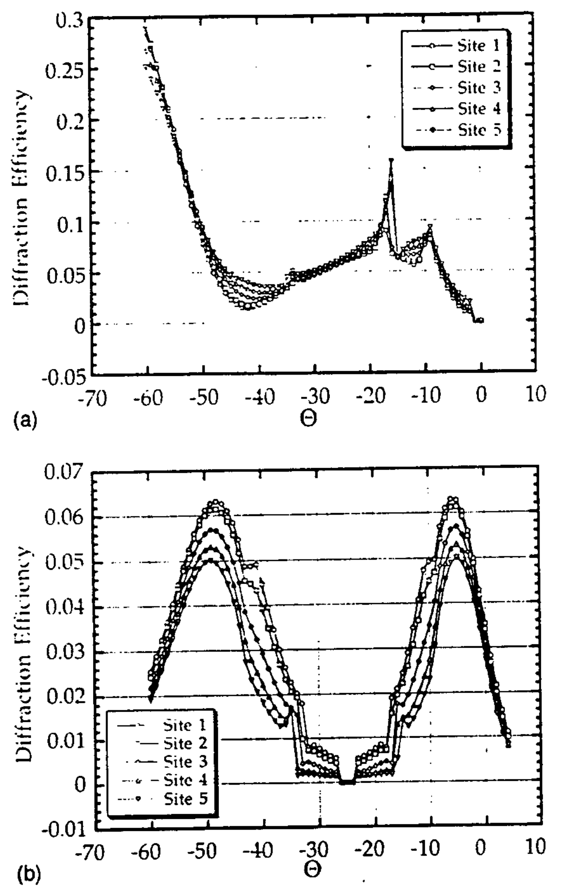

FIG. 6. Scatterometry measurements, TE conventional, at 633 nm of nominal 0.25 μm linewidth, 0.75 μm pitch photoresist-on-Si gratings, ~6 nm average linewidth increment between signatures, for (a) 0 order, (b) 1st order.

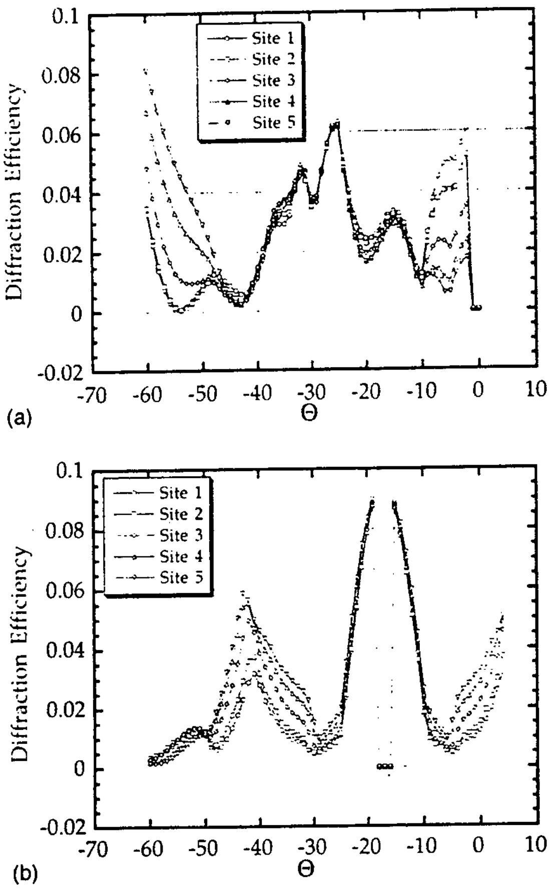

FIG. 7. Scatterometry measurements, TE conventional, at 442 nm of nominal 0.25 μm linewidth, 0.75 μm pitch photoresist-on-Si gratings, ~6 nm linewidth increment between signatures, for (a) 0 order, (b) 1st order.

## B. Sensitivity metric

In order to assess the sensitivity of the scatterometry technique at different wavelengths and for different samples, a common metric is required. We define sensitivity as the change in a measured parameter versus a change in a sample feature (e.g., linewidth). In scatterometry, the measured parameter is a point in the "scatterometer signature," which is a normalized intensity profile measured as a function of the angle of incidence of the laser beam to the sample. Hence these signatures represent a collection of many data points which characterize the change in diffraction efficiency of the sample as the angle of incidence of the illuminating laser is changed.

Quantitative, statistical measures of the overall signature change—or amount of spread between signatures corresponding to two samples having different linewidths—include range, mean absolute variation, variance, standard deviation, and mean-square error (MSE). Previously, we have used normalized MSE, an adaptation of our earlier (non-normalized) MSE computations for matching experimental data to model predictions when the two data sets are similar in range. However, the normalized MSE technique overemphasizes portions of the signature that have very small values of diffraction efficiency. A metric is desired that weights the entire signature evenly, as it is generally not known *a priori* what the shape of the experimental signature will be. To this end, we have chosen to use the average variance as the sensitivity metric, defined as

$$\overline{s^2}=\frac{1}{M}\sum_{i=1}^{M}\left[\frac{\sum_{j=1}^{n}(x_{ij}-\bar{x}_i)^2}{n-1}\right], \qquad (1)$$

where the term in brackets is recognized as the variance.[19] This term is computed by using the values of all signatures resulting from linewidth variations, i.e., $x_{ij}$ represents a diffraction efficiency for the $i$th incidence angle and the $j$th linewidth. The term preceding the brackets takes the average over all angles of incidence. This process is illustrated in Fig. 5 for three example signatures: at each angle of incidence, i.e., for $i=1,2,3...18$, the mean, $\bar{x}_i$, and a variance are computed. In this example, the number of signatures ($n$) is equal to 3, and the number of incident angles ($M$) is 18. The "average variance" is taken to be a measure of the spread between the curves, and in the following sections is referred to as "avg. variance". An average is appropriate as long as the CD increment is small, and changes are comparable in magnitude from one signature to the next. A larger value of avg. variance indicates higher measurement sensitivity, which is of value in a process metrology tool for nanometer-

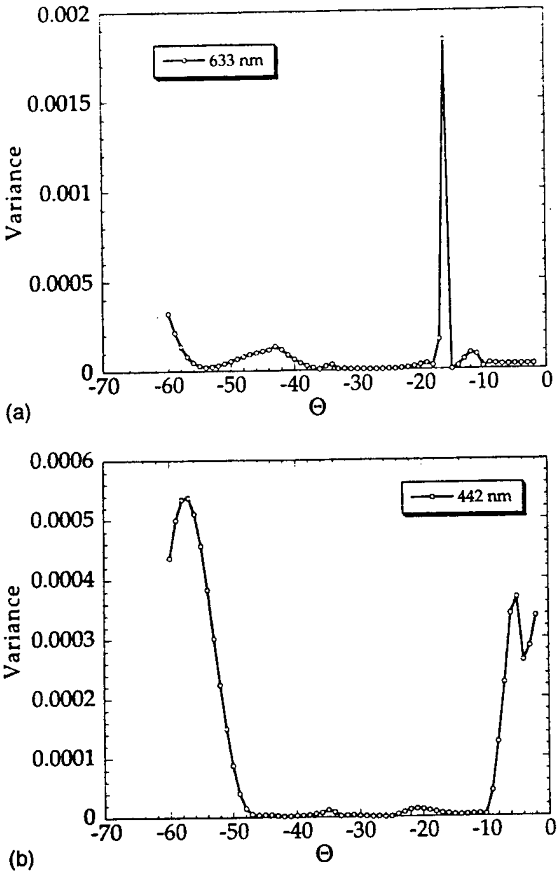

FIG. 8. Variance between signatures as a function of angle of incidence for 0-order scatterometry measurements, TE conventional, of nominal 0.25 μm linewidth, 0.75 μm pitch photoresist-on-Si gratings, ~6 nm linewidth increment between signatures, at (a) 633 nm, (b) 442 nm.

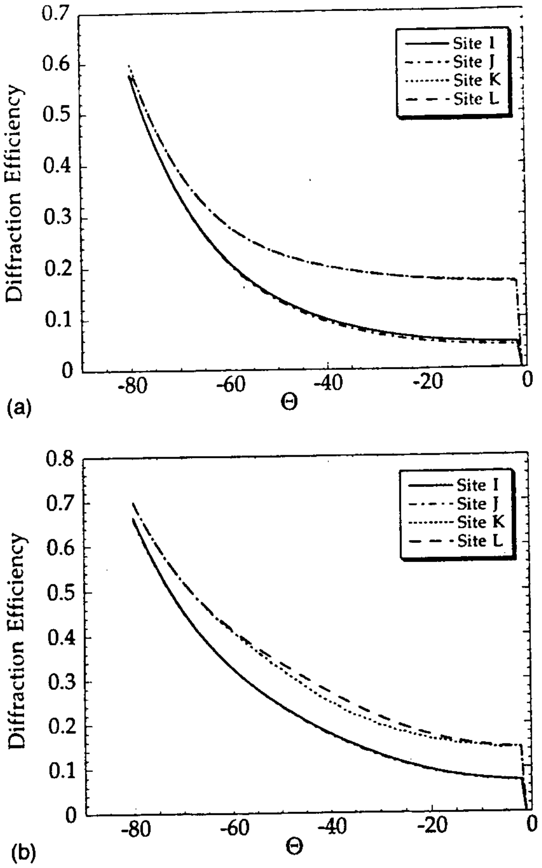

FIG. 9. Scatterometry measurements, TM conventional, of sub-0.1 μm linewidth, 0.2 μm pitch InP etched gratings, ~25 nm linewidth increment between *I*-*J* and *K*-*L* signatures, at (a) 633 nm, (b) 442 nm.

scale variations. Scatterometer signatures may exhibit considerably more structure than is shown in the example, as will be seen in the following sections.

## IV. WAVELENGTH EFFECTS ON MEASUREMENT SENSITIVITY

### A. Large-pitch samples

Initial experiments using 633 and 442 nm incident wavelengths were performed on samples obtained from SEMATECH. The samples consisted of developed photoresist patterns of nominal 0.35 μm lines, 0.80 μm pitch, and nominal 0.25 μm lines, 0.75 μm pitch. Samples with similar grating dimensions, along with conventional 633 nm scatterometer measurements, are described in detail by Raymond *et al.*[9]

Our task with this same type of grating structure was to determine whether the sensitivity of scatterometry was significantly improved by using shorter laser wavelengths. Because the pitch of these sample gratings was relatively large with respect to the operating wavelengths, both 0- and 1st-order diffraction were characterized. A typical series of measurements is shown in Figs. 6(a) and 6(b) and 7(a) and 7(b) for 633 and 442 nm laser wavelengths, respectively. Stepping from test site to test site corresponds to a linewidth increment of nominally 6 nm. The following trends can be observed from the signatures. When the pitch is large compared to the incident wavelength, as in the current example, the 1st order may show more sensitivity than the 0 order. For example, where sensitivity appears low for 633 nm in the 0-order signature [Fig. 6(a)], it is recovered in the 1st-order signatures [Fig. 6(b)]. At 442 nm, there is sensitivity in the 0 order [Fig. 7(a)] as well as in 1st-order [Fig. 7(b)] signatures. Also, it can be observed that at 442 nm there is more "structure" to the signatures, which helps to differentiate between CD increments. There is a noticeable spreading between the signatures, and this occurs at different angular locations depending upon diffraction order, wavelength, mounting configuration, and laser polarization. Applying the avg. variance sensitivity metric to the 0-order data, the resulting values are $7.95\times 10^{-5}$ for 633 nm and $1.07\times 10^{-4}$ for 442 nm, indicating a 35% sensitivity improvement at 442 nm. The individual variances used to compute the avg. variance are plotted in Figs. 8(a) and 8(b) as a function of incidence angle, Θ. These variance plots are helpful in identifying regions of maximum sensitivity as the angle of incidence is varied, again depending upon the sample and measurement details. For example, Fig. 8(a) shows a narrow region of higher sensitivity near 16° angle of incidence, while sensitivity is low at all other angles. At 442 nm, as shown in Fig. 8(b), two broader regions of sensitivity are indicated, from 2° to 8° and

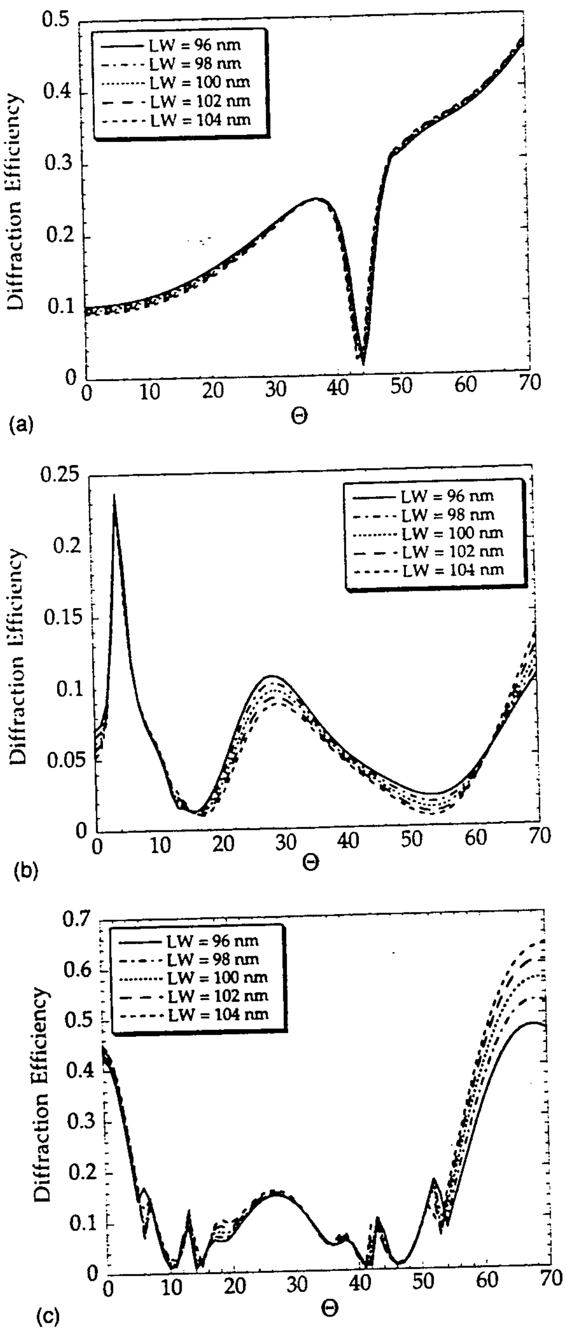

FIG. 10. Scatterometry model results, TE conventional, for nominal 0.1 $\mu$m linewidth, 0.36 $\mu$m pitch photoresist-on-ARC-on-Si gratings, 2 nm linewidth increment between signatures, at (a) 633 nm, (b) 442 nm, (c) 325 nm.

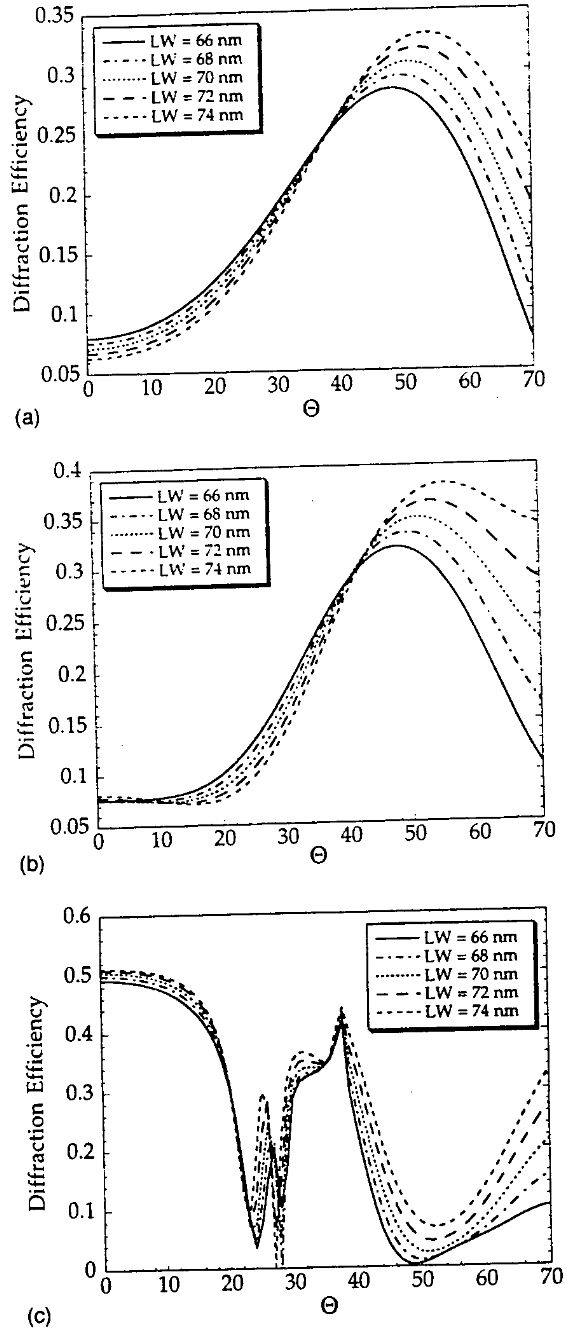

FIG. 11. Scatterometry model results. TE conventional, for nominal 0.07 $\mu$m linewidth, 0.2 $\mu$m pitch photoresist-on-ARC-on-Si gratings, 2 nm linewidth increment between signatures, at (a) 633 nm, (b) 442 nm, (c) 325 nm.

above 50°. These observations are consistent with the subjective assessment of signature "spreading" as linewidth is varied, as discussed in connection with Figs. 6(a) and 7(a). Having developed and tested a sensitivity metric, it was desired to investigate shorter-pitch grating samples with sub-0.1 $\mu$m linewidths.

## B. Short-pitch samples

The samples of etched InP gratings previously mentioned in connection with Figs. 3 and 4 were used for this investigation. Although not representative of Si technology in terms of material or dimensions, these were the only uniform, well-characterized sub-0.1 $\mu$m CD samples available. The nominal grating pitch was 0.2 $\mu$m, with linewidths ranging from 25 to 55 nm, and depths of 100 to 200 nm. Because this pitch is considerably smaller than the incident wavelength, the grating only produces 0-order diffraction at 633 and 442 nm wavelengths. Scatterometer signatures for the TM-conventional mounting mode are shown in Figs. 9(a) and 9(b) for the two wavelengths, respectively. A computation resolution of 2 nm was used, and the nominal CD increment on the wafer was 25 nm in this case. The avg. variances for

TABLE I. Summary of avg. variances for all configurations vs $\lambda_0$, for 100 nm lines.

| $\lambda_0$ | Conventional | | Conic | |
|---|---|---|---|---|
| (nm) | TE | TM | TE | TM |
| 633 | 4.3e−5 | 1.0e−5 | 4.5e−5 | 9.8e−6 |
| 442 | 3.0e−5 | 1.0e−5 | 4.4e−5 | 3.0e−5 |
| 325 | 7.0e−4 | 7.1e−4 | 1.6e−3 | 2.7e−4 |

these signatures are $4.40\times10^{-3}$ at 633 nm and $2.47\times10^{-3}$ at 442 nm, showing no significant influence on the sensitivity by using the shorter measurement wavelength. Note, however, that scatterometry, even at the 633 nm incident wavelength, exhibits sufficient sensitivity to remain a useful tool for detecting changes in linewidth in the 0.05 μm CD region.

Overall sensitivity can be compared to those levels reported above for large-pitch samples by dividing the large- and short-pitch avg. variance metrics by the respective linewidth increments in each case, yielding a variance-per-nm figure. At 633 nm wavelength, the result is $1.3\times10^{-5}$ $\mathrm{nm}^{-1}$ for the large-pitch sample and $1.8\times10^{-4}$ $\mathrm{nm}^{-1}$ for the short-pitch sample. At 442 nm, the result is $1.8\times10^{-5}$ $\mathrm{nm}^{-1}$ for the large-pitch sample and $9.9\times10^{-5}$ $\mathrm{nm}^{-1}$ for the short-pitch sample. At both wavelengths, somewhat greater sensitivity per nm was observed with the short-pitch sample. Such a result is surprising if one considers that as the linewidth and pitch of the grating are reduced below the incident wavelength, $\lambda_0$, these features have less and less effect and begin to approximate a surface roughness on a scale $\ll\lambda_0$. This result quite possibly is due to the dissimilar materials and dimensions between the photoresist-on-Si and the etched InP samples and suggests that other factors, in addition to wavelength, also influence sensitivity. Hence, we do not regard the differences in sensitivity shown with these dissimilar samples to be noteworthy. Experimentally, we have observed that the structure, or variation, within diffraction signatures tends to disappear as the pitch and linewidth are reduced. Note the Fresnel-like characteristics of the short-pitch InP samples in Fig. 9(a), as compared to the less-predictably varying large-pitch signatures in Fig. 6(a). In Fig. 10, one observes that the signatures contain more structure as the incident wavelength is reduced.

### C. Modeling of sub-0.1 μm photoresist-on-silicon gratings

To assess the measurement sensitivity for a short-pitch photoresist structure with dimensions consistent with Technology Roadmap projections, the diffraction of nominal 70 and 100 nm linewidth photoresist grating structures on Si was investigated using computer modeling; well-characterized samples were not available for actual measurements. The grating pitches were fixed at 0.20 and 0.36 μm, respectively. Resist height was 0.5 μm, and an anti-reflection layer (ARC) of 75 nm was included between the resist and the Si substrate. Diffraction from these structures was evaluated at laser wavelengths of 633, 442, and 325 nm, and the refractive indices for resist, ARC and Si, were set corresponding to each wavelength. Five linewidth steps in increments of 2 nm were modeled at each wavelength: nominal linewidth, nominal ±2 nm, and nominal ±4 nm.

TABLE II. Summary of avg. variances for all configurations vs $\lambda_0$, for 70 nm lines.

| $\lambda_0$ | Conventional | | Conic | |
|---|---|---|---|---|
| (nm) | TE | TM | TE | TM |
| 633 | 5.1e−4 | 2.4e−6 | 1.3e−4 | 3.5e−5 |
| 442 | 1.1e−3 | 2.0e−5 | 7.7e−5 | 2.5e−5 |
| 325 | 1.6e−3 | 6.9e−4 | 4.1e−4 | 2.0e−4 |

A representative set of signatures, in this case for the TE-conventional measurement configuration, are shown in Figs. 10(a)–10(c) and 11(a)–11(c) for the nominal 100 and 70 nm linewidths, respectively. Tables I and II summarize the sensitivity metric data for the 100 and 70 nm cases, respectively, for the four combinations of TE/TM input polarization and conventional/conical grating mounting.

These avg. variance data are plotted in Figs. 12(a) and 12(b). Qualitatively, it can be observed in Figs. 10 and 11 that the spreading between signatures increases for decreasing incident wavelength. The metric plots of Fig. 12 indicate, however, that the benefit in sensitivity is not pronounced

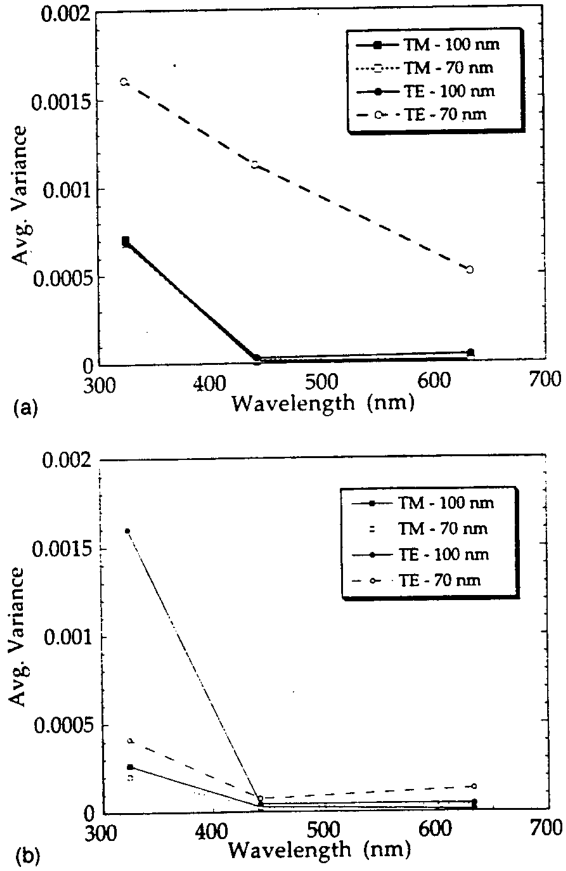

FIG. 12. Avg. variance as a function of wavelength from scatterometry model results, for nominal 0.07 and 0.1 μm linewidths, photoresist-on-ARC-on-Si gratings, for (a) TE and TM conventional, (b) TE and TM conic.

until the wavelength is reduced to 325 nm. An exception to this trend is observed for the TE-conventional case for nominal 70 nm linewidths, as shown in Fig. 12(a). The increase in sensitivity for this particular configuration may be related to the pitch of the grating and is an area requiring further investigation. The implication is that there may be ways of increasing the scatterometry measurement sensitivity by careful selection of test grating dimensions. Prefabrication modeling would allow an optimum test structure to be designed.

## V. CONCLUSIONS

In response to the need to assess measurement sensitivity, an avg. variance metric was developed. This metric was then used to compare scatterometer measurement sensitivity at multiple wavelengths, to determine angular regions of sensitivity, and to gain insight into the influence of other parameters on measurement sensitivity.

When the pitch of the sample is large compared to the incident wavelength, the 1st order may be useful, i.e., where sensitivity is low for the 0-order signature, it possibly may be recovered in the 1st order. At 442 nm there was still significant sensitivity at 0 order and at 1st order, and there was more structure to the signatures, which helps to differentiate between CD increments. For shorter-pitch structures for which only a 0-order diffraction signature is possible, structure in the signature is reduced, but the signature still exhibits its sensitivity to linewidth variations when using the 633 nm incident wavelength.

From these data, it can be concluded that the strategy of reducing the scatterometer operating wavelength may increase sensitivity significantly, particularly at the 325 nm wavelength. However, such an improvement is quite dependent on the sample materials involved and the grating test structure. For photoresist grating structures on Si, it appears that scatterometry measurement sensitivity can be positively influenced by judicious selection of test structure dimensions. We are presently investigating additional techniques for increasing measurement sensitivity for sub-0.1 μm structures while maintaining use of the convenient 633 nm laser wavelength.

## ACKNOWLEDGMENTS

Wafer samples and SEM/AFM measurements used in these studies were provided by SEMATECH and Lucent Technologies. The authors thank SRC and ARPA for partial financial support of this work.

[1] H. P. Kleinknecht and H. Meier, J. Electrochem. Soc. **125**, 798 (1978).
[2] H. P. Kleinknecht and H. Meier, Appl. Opt. **19**, 525 (1980).
[3] M. G. Moharam and T. K. Gaylord, J. Opt. Soc. Am. **72**, 1385 (1982).
[4] J. R. McNeil, S. S. H. Naqvi, S. M. Gaspar, K. C. Hickman, K. P. Bishop, L. M. Milner, R. H. Krukar, and G. A. Petersen, Microlithography World **1**, 16 (1992).
[5] S. S. H. Naqvi, J. R. McNeil, R. H. Krukar, and K. P. Bishop, Microlithography World **2**, 5 (1993).
[6] R. H. Krukar, S. L. Prins, D. M. Krukar, G. A. Petersen, S. M. Gaspar, J. R. McNeil, S. S. H. Naqvi, and D. R. Hush, Proc. SPIE **1926**, 60 (1993).
[7] M. R. Murnane, C. J. Raymond, S. S. H. Naqvi, and J. R. McNeil, Proc. SPIE **2532**, 251 (1995).
[8] C. J. Raymond, M. R. Murnane, S. S. H. Naqvi, and J. R. McNeil, J. Vac. Sci. Technol. B **13**, 1484 (1995).
[9] C. J. Raymond, M. R. Murnane, S. L. Prins, S. S. H. Naqvi, and J. R. McNeil, J. Vac. Sci. Technol. B **15**, 361 (1997).
[10] J. Bishoff, J. W. Baumgart, and H. Truckenbrodt, Proc. SPIE **2725**, 678 (1996).
[11] *The National Technology Roadmap for Semiconductors* (Semiconductor Industry Association, San Jose, 1994).
[12] R. Iscoff, Semicond. Int. **17**, 56 (1994).
[13] D. Nyyssonen and R. D. Larrabee, NBS J. Res. **92**, 187 (1987).
[14] C. J. Raymond, J. R. McNeil, and S. S. H. Naqvi, Proc. SPIE **2725**, 720 (1996).
[15] S. L. Prins, L. M. Milner, S. H. Zaidi, S. S. H. Naqvi, and J. R. McNeil, SRC TECHON 93 Extended Abstracts 447 (1993).
[16] E. Yoon, C. A. Green, R. A. Gottscho, T. R. Hayes, and K. P. Giapis, J. Vac. Sci. Technol. B **10**, 2230 (1992).
[17] B. Minhas, S. L. Prins, S. S. H. Naqvi, and J. R. McNeil, Proc. SPIE **2725**, 729 (1996).
[18] T. K. Gaylord and M. G. Moharram, Proc. IEEE **73**, 894 (1985).
[19] M. Hamburg, *Statistical Analysis for Decision Making* (Harcourt Brace Jovanovich, New York, 1977), p. 39.

TECHNICAL NOTE

# Ellipsometric scatterometry for the metrology of sub-0.1-μm-linewidth structures

Babar K. Minhas, Stephen A. Coulombe, S. Sohail H. Naqvi, and John R. McNeil

We describe a modification to our existing scatterometry technique for extracting the relative phase and amplitude of the electric field diffracted from a grating. This modification represents a novel combination of aspects of ellipsometry and scatterometry to provide improved sensitivity to small variations in the linewidth of subwavelength gratings compared with conventional scatterometer measurements. We present preliminary theoretical and experimental results that illustrate the possibility of the ellipsometric scatterometry technique providing a metrology tool for characterizing sub-0.1-μm-linewidth. © 1998 Optical Society of America

*OCIS codes:* 050.1950, 050.1960, 050.2770, 120.2130, 120.3940, 120.5820.

## 1. Introduction

Scatterometry,[1] defined as the angle-resolved characterization and analysis of light, is an attractive metrology technique for determining grating profiles. Previous research has demonstrated the use of scatterometry for characterizing 0.2–0.4-μm grating lines with a 0.75-μm pitch.[2] These lines were characterized within a computational resolution of ±10 nm. However, devices having linewidths of the order of 0.12 μm are expected in the near future, and metrology techniques will be required for detecting changes as small as ~1 nm.[3] The measurement sensitivity of conventional scatterometry techniques, utilizing a 633-nm-wavelength light to illuminate the sample, decreases for samples having linewidths of ≤0.1 μm and pitches of ≤0.3 μm. To illustrate this concern, consider the case of a 0.2-μm-pitch InP grating with a grating height of 0.1 μm. Figure 1 shows the theoretical diffraction signature of the grating for linewidths of 96, 98, and 100 nm. As can be seen from the figure, the changes in the diffraction efficiencies are barely noticeable, making the technique incapable of characterizing linewidth variations of 2 nm in this case. To enhance diffraction sensitivity, we have exploited the grating geometry by using it in a conical configuration.[4] Although this improves the diffraction sensitivity to linewidth variations, the improvement is not sufficient to ensure the uniqueness of the diffraction signature. Another approach to improving the resolution of the scatterometer method is to use shorter illuminating wavelengths. To this end we have explored the use of a HeCd laser (λ = 442 nm) for characterizing sub-0.1-μm linewidth structures. Our experimental and theoretical studies show that significant improvement in sensitivity is not achieved until the wavelength of the illuminating beam is in the ultraviolet spectrum.[5] Using ultraviolet light for scatterometry currently is not as practical as using visible wavelengths because of the added complexity of the experimental arrangement.

Our goal therefore has been to extract more information from the diffracted light by using a convenient illuminating wavelength, such as from a He–Ne laser. This is accomplished by incorporating features of ellipsometry with scatterometry to extract phase information. This modified scatterometry technique continues to employ the matching of experimental scatter signatures with theoretical signatures produced with computational techniques. In this note we describe the modifications that we have made in our existing scatterometer to this end. These changes show the promise of characterizing linewidth variations as small as ~1 nm.

## 2. Experimental Arrangement

Using the notation of Ref. 6, let ($\mathbf{E}_{ip}$, $\mathbf{E}_{is}$) and ($\mathbf{E}_{rp}$, $\mathbf{E}_{rs}$) represent the complex electric-field vectors of the

---

The authors are with the Center for High Technology Materials, University of New Mexico, Albuquerque, New Mexico 87131. S. S. H. Naqvi is also with the GIK Institute of Engineering Science and Technology, Pakistan.

Received 5 November 1997; revised manuscript received 27 March 1998.

0003-6935/98/225112-04$15.00/0

© 1998 Optical Society of America

incident and the reflected fields, respectively. The ellipsometric parameter ρ is then defined as

$$\rho = (E_{rp}/E_{ip})/(E_{rs}/E_{is}) = \tan\Psi \exp(i\Delta). \qquad (1)$$

Our experimental approach is to extract these ellipsometric parameters Ψ and Δ from intensity measurements, and for the purpose of this investigation we are not extracting the sign of Δ. This approach was used previously by Beattie[7] for studying optical constants of metals in the IR spectrum. Figure 2 shows the ellipsometric scatterometer. A TE-polarized He–Ne laser is used as the source of illumination. The incident beam passes through the polarizer, which has its transmission axis at angle $P$ with respect to the horizontal plane, and illuminates the grating. The grating can be rotated about the vertical axis to provide θ variations and about the normal to the sample plane to provide ϕ variations. Since we are primarily characterizing gratings having periods that are much smaller than the illuminating wavelength, the only propagating order in air is the 0 order. The beam diffracted in the 0 order is passed through an analyzer having a transmission axis at angle $A$ with respect to the horizontal plane and then to the photodetector.

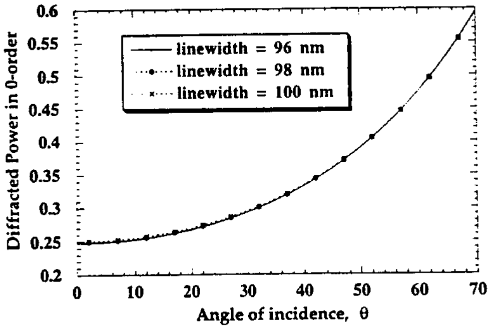

Fig. 1. Lack of diffraction sensitivity to linewidth variations for conventional scatterometer simulations for a 0.2-μm-pitch InP grating with a binary profile: grating height, 0.1 μm; illuminating beam, TE-polarized He–Ne laser (λ = 633 nm).

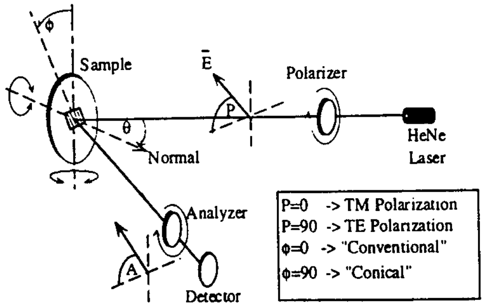

Fig. 2. Ellipsometric scatterometer arrangement.

Currently we are mounting the grating with the grating lines either parallel (ϕ = 0°) or normal (ϕ = 90°) to the vertical axis. We keep the polarizer angle $P$ fixed, and for a given value of the analyzer angle $A$ we vary θ in steps of 1 deg to characterize the 0-order diffraction. We show in Section 3 that for any value of θ, taking data for $A$ = 0°, 45°, and 90° is sufficient to extract Ψ and |Δ| of the diffracted field.

## 3. Analysis

We use Jones calculus to analyze the change in polarization of the incident beam as it propagates through the optical system. The Jones matrices for the configuration illustrated in Fig. 2 are given by

$$\begin{bmatrix} \mathbf{E}_x \\ \mathbf{E}_y \end{bmatrix} = \underbrace{\begin{bmatrix} \cos^2 \mathbf{A} & \cos \mathbf{A} \sin \mathbf{A} \\ \cos \mathbf{A} \sin \mathbf{A} & \sin^2 \mathbf{A} \end{bmatrix}}_{[\mathbf{A}]} \times \underbrace{\begin{bmatrix} \mathbf{R}_{pp} & \mathbf{R}_{ps} \\ \mathbf{R}_{sp} & \mathbf{R}_{ss} \end{bmatrix}}_{[\mathbf{R}]} \times \underbrace{\begin{bmatrix} \cos^2 \mathbf{P} & \cos \mathbf{P} \sin \mathbf{P} \\ \cos \mathbf{P} \sin \mathbf{P} & \sin^2 \mathbf{P} \end{bmatrix}}_{[\mathbf{P}].} \begin{bmatrix} 0 \\ 1 \end{bmatrix} \qquad (2)$$

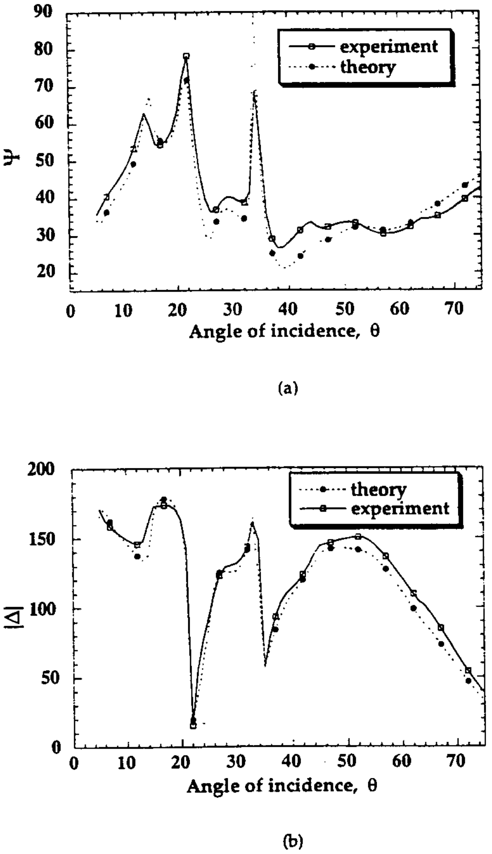

(a)

(b)

Fig. 3. Comparison of experiment versus theory for a 1.0-μm developed photoresist grating ($n$ = 1.576, $k$ = 0.001) on a Si substrate. The grating has a binary profile with a linewidth of 0.53 μm and height of 1.0 μm. The incident beam is linearly polarized with $P$ = 45° and is from a He–Ne laser (λ = 633 nm). The grating is mounted in classical configuration, i.e., ϕ = 0°: (a) Ψ versus incidence angle θ; (b) |Δ| versus incidence angle θ.

Here [**P**] and [**A**] are matrices that characterize the polarizer and the analyzer, respectively.[8] The [**R**] matrix characterizes the grating and its nonzero, off-diagonal elements show that polarization conversion of the incident beam takes place as part of diffraction from the grating. The (complex) elements $R_{ps}$ and $R_{sp}$ are always zero for $\phi = 0°$ and $\phi = 90°$; no polarization conversion takes place.

Evaluating Eq. (2) for the cases of $\phi = 0°$ and $\phi = 90°$, we express the intensity of the 0-order diffracted beam $I(A, P, \theta)$ as

$$\begin{aligned} I(A, P, \theta) = {} & (\cos \mathbf{P} \sin \mathbf{P} |\mathbf{R}_{pp}| \cos \mathbf{A})^2 \\ & + (\sin^2 \mathbf{P} |\mathbf{R}_{ss}| \sin \mathbf{A})^2 \\ & + \cos \mathbf{P} \sin^3 \mathbf{P} |\mathbf{R}_{pp}||\mathbf{R}_{ss}| \cos(\Delta) \sin 2\mathbf{A}. \end{aligned} \quad (3)$$

When we evaluate Eq. (3) for $P = 45°$ and $A = 0°, 45°, 90°, 135°$, $I(A, P, \theta)$ becomes

$$\mathbf{I}(0°, 45°, \theta) = |\mathbf{R}_{pp}|^2/4, \quad (4)$$

$$\begin{aligned} \mathbf{I}(45°, 45°, \theta) = {} & 1/4[(|\mathbf{R}_{pp}|^2 + |\mathbf{R}_{ss}|^2)/2 \\ & + |\mathbf{R}_{pp}||\mathbf{R}_{ss}| \cos(\Delta)], \end{aligned} \quad (5)$$

$$\mathbf{I}(90°, 45°, \theta) = |\mathbf{R}_{ss}|^2/4, \quad (6)$$

$$\begin{aligned} \mathbf{I}(135°, 45°, \theta) = {} & 1/4[(|\mathbf{R}_{pp}|^2 + |\mathbf{R}_{ss}|^2)/2 \\ & - |\mathbf{R}_{pp}||\mathbf{R}_{ss}| \cos(\Delta)]. \end{aligned} \quad (7)$$

Although the first three expressions are sufficient to determine $\Psi$ and $|\Delta|$, we also use the fourth to improve experimental accuracy.

## 4. Comparison of Theory and Experiment

We used a rigorous coupled wave analysis,[9] an important part of the scatterometry technique, to calculate the elements of the [**R**] matrix and measured the developed photoresist gratings to verify the theoretical analysis described in Section 3. Figure 3 shows experimental and theoretical results for a developed photoresist grating having a pitch of 1.0 μm and a linewidth of 0.53 μm. Raymond *et al.*[10] have previously characterized this grating by extensively using conventional scatterometry and SEM measurements. As may be seen from Fig. 3, the theoretical and the experimental data are in good agreement.

Owing to the unavailability of suitable sub-0.1-μm structures, we were not able to demonstrate experimentally the sensitivity of the ellipsometric scatterometry technique. However, we carried out theoretical simulations to verify the diffraction sen-

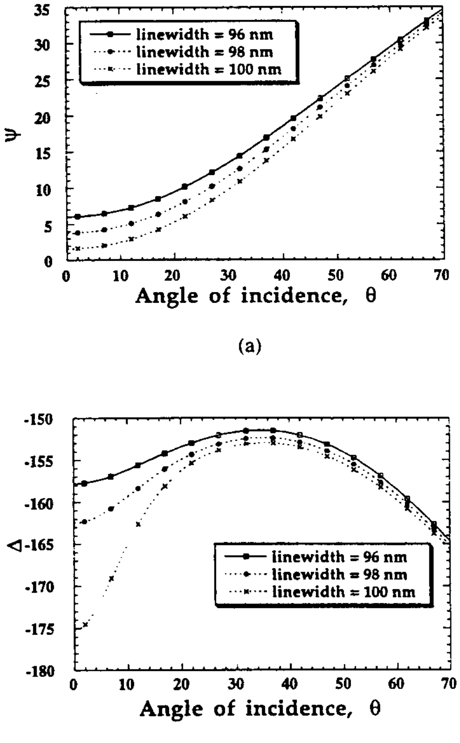

(a)

(b)

Fig. 4. Numerical modeling results from using rigorous coupled-wave analysis showing diffraction sensitivity to 2-nm-linewidth variations for a 0.2-μm-pitch InP grating. The grating is assumed to have a binary profile with a height of 0.1 μm. The illuminating beam is linearly polarized with $P = 45°$ and $\lambda = 633$ nm. The grating is mounted in a classical configuration, i.e., $\phi = 0°$: (a) $\Psi$ versus incidence angle $\theta$; (b) $\Delta$ versus incidence angle $\theta$.

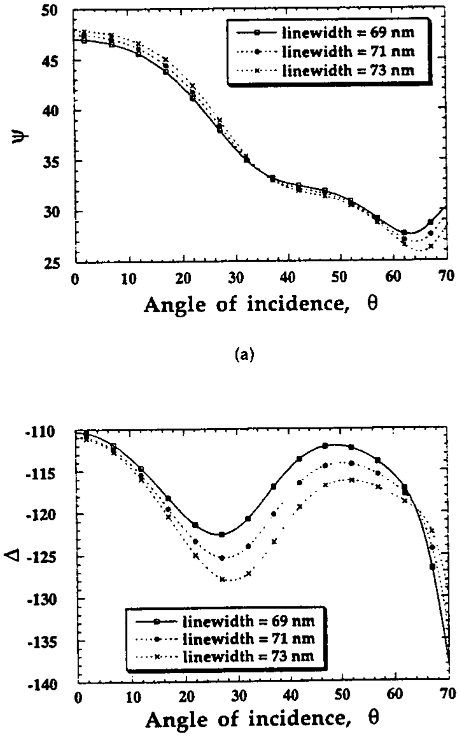

(a)

(b)

Fig. 5. Numerical modeling results from using rigorous coupled-wave analysis showing diffraction sensitivity to 2-nm-linewidth variations for a 0.2-μm-pitch developed photoresist grating ($n = 1.576$) on a Si substrate. The grating is assumed to have a binary profile with a height of 0.7 μm. The illuminating beam is linearly polarized with $P = 45°$ and $\lambda = 633$ nm. The grating is mounted in a conical configuration with $\phi = 90°$: (a) $\Psi$ versus incidence angle $\theta$; (b) $\Delta$ versus incidence angle $\theta$.

sitivity of the technique. These simulations were based on rigorous coupled wave analysis[9] and the ellipsometric parameters $\Psi$ and $\Delta$ as defined above in Eq. (1). Figure 4 shows the $\Psi$ and $\Delta$ variation versus angle of incidence $\theta$ for the 0.2-μm-pitch InP grating discussed in connection with Fig. 1. As expected, parameters $\Psi$ and $\Delta$, determined through modified scatterometry, are significantly more sensitive to the 2-nm-linewidth variations than the conventional scatterometer measurements illustrated in Fig. 1. The measurements can resolve 2-nm variations in a sample linewidth. Similarly, Fig. 5 shows $\Psi$ and $\Delta$ variations versus angle of incidence $\theta$ for 0.2-μm-pitch developed photoresist gratings on Si. These simulations were also performed to characterize linewidth variations of 2 nm. Again we note that changes in the diffracted light parameters, $\Psi$ and $\Delta$, are sufficient to detect 2-nm variations in linewidths.

## 5. Conclusion

We have demonstrated the feasibility of ellipsometric scatterometry for the metrology of sub-0.1-μm linewidth structures. This technique, compared with conventional scatterometry, exploits additional phase information of the diffracted light, which is sensitive to grating linewidth variations. The technique permits an accurate characterization of sub-0.1-μm linewidths with ~1-nm precision.

The authors thank DARPA (Defense Advanced Research Projects Agency) and the Semiconductor Research Corporation for partial financial support of this research and Lucent Technologies for providing 0.2-μm-pitch samples.

## References

1. S. S. H. Naqvi, J. R. McNeil, R. H. Krukar, and K. P. Bishop, "Scatterometry and the simulation of diffraction-based metrology," Microlithogr. World **2**(3), 5–16 (1993).
2. C. J. Raymond, M. R. Murnane, S. L. Prins, S. S. H. Naqvi, J. W. Hosch, and J. R. McNeil, "Multiparameter grating metrology using optical scatterometry," J. Vacuum Sci. Technol. B **15,** 361–368 (1997).
3. *The National Technology Roadmap for Semiconductors* (Semiconductor Industry Association, San Jose, Calif., 1994).
4. B. K. Minhas, S. L. Prins, S. S. H. Naqvi, and J. R. McNeil, "Toward sub-0.1-μm CD measurements using scatterometry," in *Integrated Circuit Metrology, Inspection, and Process Control X*, S. K. Jones, ed., Proc. SPIE **2725,** 729–739 (1996).
5. S. A. Coulombe, B. K. Minhas, C. J. Raymond, S. S. H. Naqvi, and J. R. McNeil, "Scatterometry measurement of sub-0.1-μm linewidth gratings," submitted to J. Vacuum Sci. Technol. B (1998).
6. R. M. A. Azzam and N. M. Bashara, *Ellipsometry and Polarized Light*. (North-Holland, Amsterdam, 1977).
7. J. R. Beattie, "Optical constants of metals in the infra-red—experimental methods," Philos. Mag. **46,** 235–245 (1955).
8. E. Collett, *Polarized Light—Fundamentals and Applications* (Marcel Dekker, New York, 1993).
9. M. G. Moharam and T. K. Gaylord, "Three-dimensional vector coupled-wave analysis of planar-grating diffraction," J. Opt. Soc. Am. **73,** 1105–1112 (1983).
10. C. J. Raymond, M. R. Murnane, S. S. H. Naqvi, and J. R. McNeil, "Metrology of subwavelength photoresist gratings using optical scatterometry," J. Vacuum Sci. Technol. B **13,** 1484–1495 (1995).